

POLITECNICO DI TORINO

Master's Degree in Mechanical Engineering



Master's Degree Thesis

Development of a fuel cell electric boat for an international energy challenge

Supervisors

Prof. Ezio SPESSA

Prof. Petter DAHLANDER

Prof. David SEDARSKY

Candidate

Alessandro ASTEGIANO

October 2023

Abstract

In recent years, fossil fuels have dominated the energy sector, having almost monopoly power generation in both power plants and in all means of transportation. Currently, significant legislation has been enacted to reduce greenhouse gases and pollutant emissions generated by combustion of fossil fuels. Among the proposed alternative energy sources, hydrogen-powered fuel cells are particularly appealing since they have zero local emissions. The Monaco Boat energy challenge was created to foster innovative applications to boat propulsion, with the only requirement of being carbon free. In this work, the powertrain of a fuel cell electric boat was modelled, using a multi-physics simulation software (Simcenter Amesim), starting from scratch. The fuel cell system has been modeled with distinct sub-models for the stack and auxiliary systems such as the hydrogen and air supply system, the coolant system and the control system. Furthermore, the electrical plant was modelled, including the fuel cell auxiliaries' drives and the propulsion electric motor. Then, the powertrain was modelled, including the drive shaft, transmission gears and the propeller of the boat. Finally, the boat resistance model was modelled. After integrating all sub-models into a single simulation model for the boat, an effective energy management strategy was developed in order to complete successfully all the race trials. The main outcome of this work is to build the first step toward a model that could simulate an effective race condition; the developed model can be used to investigate preliminary design variants and to rationally define the powertrain components requirements. This in turn enables an optimized selection of the powertrain components, whose data will be then used to fully characterize the developed model.

Acknowledgements

I use this chapter to say a huge thanks to everyone who was important for me in the realization of this project and in the university years. I'd like to thank professor Petter Dahlander, the one who created the whole opportunity to go abroad, in an amazing country and in an amazing university. Then I thank professor David Sedarsky, the person who gave me a hope, after the first project was cancelled, with maybe the best possible thesis project that I could dream for my interests. Thanks to the whole Chalmers fuel cell team, who helped me every time I need, always with a smile. And thanks to Malin Larsson, who helped me in every not technical aspect of my thesis and life in the university.

In seguito vorrei ringraziare il professor Ezio Spessa, che mi ha seguito per tutto il periodo di tesi, sempre disponibile a darmi una mano con affabilità e gentilezza. Ringrazio anche Federico Miretti, che mi ha aiutato con la stesura finale della tesi e mi ha fornito consigli mirati.

Detto questo, il grazie più grande va sicuramente ai miei genitori, Silvana e Marco, che mi hanno permesso di arrivare fin qui, sostenendomi e incoraggiandomi lungo tutto il mio percorso di studi. Un saluto va a tutti i miei nonni, che, anche se non sono più fisicamente a sostenermi, li sento sempre vicini. Esattamente come sento vicine quelle che ormai sono diventate mie sorelle, Erika e Camilla: grazie per avermi regalato, e regalarmi tutt'ora, un sorriso ogni volta che tornavo a casa. Uscendo dal mio nucleo familiare, volevo sentitamente ringraziare tutti coloro i quali mi hanno accompagnato in questo lungo periodo universitario, in particolare le famiglie Riva e Vargiu tutte. Un grazie a tutti i miei amici, sia quelli che mi hanno fatto svagare quando il mio cervello era saturo di formule, sia Andrea e Giuseppe, con cui ho passato 5 anni di università stupendi, pieni di studio, ilarità e allegria.

Table of Contents

List of Tables	VI
List of Figures	VII
Acronyms	X
1 From fossil fuels to hydrogen	1
1.1 The carbon fuel dominion	1
1.2 The decarbonization path	7
1.3 An alternative fuel: hydrogen	8
1.4 Hydrogen internal combustion engine	11
1.5 Hydrogen fuel cell	14
2 The Monaco energy boat challenge	23
2.1 Energy class rules	23
3 The fuel cell model	26
3.1 The software Simcenter Amesim	26
3.2 Gases and materials definitions	27
3.3 Fuel cell stack model	28
3.4 Air supply system	30
3.5 Hydrogen supply system	33
3.6 Cooling system	35
3.7 Electrical system	37
3.8 Control system	39
4 Boat propulsion system	45
4.1 Electric motor	46
4.2 Boat drivetrain	46
4.3 Boat resistance model	50

5	Model design through the three trials	55
5.1	The maneuverability test	55
5.2	The endurance test	57
5.3	One lap race	64
6	Conclusions	68
6.1	Results	68
6.2	Future developments	69
	Bibliography	71

List of Tables

1.1	Hydrogen properties[1]	8
2.1	Boat main dimensions[7]	24
3.1	Fuel cell datasheet [10]	28
4.1	Electric motor performances	46
4.2	Propeller main parameter	48
4.3	Main dimensions of the Amesim boat model	50

List of Figures

1.1	liquid fuel systems volumes	2
1.2	fuels gravimetric and volumetric density	2
1.3	PFI injection system	3
1.4	GDI injection system	3
1.5	Gasoline injector	4
1.6	Diesel injection system	5
1.7	Diesel injector	6
1.8	Bipolar plates[1]	10
1.9	Hydrogen outward injector[5]	13
1.10	Outward and inward hydrogen injector[3]	13
1.11	Fuel cell reactants and products[6]	15
1.12	Energy of reactants and products of a fuel cell[6]	15
1.13	Fuel cell voltage losses[6]	18
1.14	Fuel cell operating curve[6]	19
1.15	Comparison between engines and fuel cells[6]	22
2.1	Speed trial course[8]	24
3.1	Materials, gases and liquids definition	28
3.2	Polarization curve [10]	29
3.3	Oxygen supply system scheme	30
3.4	Air supply system model	32
3.5	Hydrogen supply system scheme	33
3.6	Hydrogen supply system model	35
3.7	Cooling system scheme	35
3.8	Cooling system model	37
3.9	Electrical system scheme	38
3.10	Electric motor Amesim component	39
3.11	Transmitter of current signal model	40
3.12	Oxygen control system model	41
3.13	Hydrogen control system	42

3.14	Cooling system control model	43
4.1	Propulsion system scheme	45
4.2	Sea water properties definition	45
4.3	Boat drivetrain drawing	47
4.4	Boat drivetrain model	48
4.5	Four quadrants diagram [9]	49
4.6	Powertrain model	50
4.7	Boat resistance of the Amesim model	51
4.8	Wetted surface coefficient[14]	53
4.9	Calculated boat resistance	53
5.1	Slalom trial course[8]	55
5.2	Inverter-reducer gear ratio	56
5.3	Boat speed in a maneuverability simulation	56
5.4	Endurance race path[8]	57
5.5	Solar panels model	59
5.6	Endurance race simulation, fuel cell power	60
5.7	Endurance race simulation, hydrogen flow rate	60
5.8	Endurance race simulation, recirculation and purge	61
5.9	Endurance race simulation, stack temperature	61
5.10	Endurance race simulation, temperature of coolant at the inlet and outlet from the radiator	62
5.11	Endurance race simulation, fan activation phases	62
5.12	Endurance race simulation, air flow rate	63
5.13	Endurance race simulation, boat speed	63
5.14	Championship race, fuel cell power	64
5.15	Championship race, hydrogen flow rate at fuel cell inlet	65
5.16	Championship race, stack temperature	65
5.17	Championship race, temperature of coolant at the inlet and outlet from the radiator	66
5.18	Championship race, air speed increase because of the fan	66
5.19	Championship race, air flow rate	67
5.20	Championship race, boat speed	67

Acronyms

B

BTE brake thermal efficiency

D

DOC Diesel oxidation catalyst

DPF Diesel particulate filter

E

ECU electronic central unit

EGR exhaust gas recirculation

G

GDI gasoline direct injection

GDL gas diffusion layer

GHG greenhouse gases

H

HC unburnt hydrocarbons

I

ICE internal combustion engine

IVC intake valve closing

IVO intake valve opening

L

LP-DI low pressure direct injection

N

NMOG non-methane organic gas

P

PFI port fuel injection

PI proportional integral

PM particulate matter

S

SCR selective catalytic reduction

T

TWC 3-way catalyst

W

WGS water-gas shift

Chapter 1

From fossil fuels to hydrogen

1.1 The carbon fuel dominion

The invention of the internal combustion engine (ICE) has revolutionized how people and goods could move. The most advanced technology was the steam engine, but the discovery of petroleum changed the world; the researches of Otto (in 1867) and Diesel (in 1893) made a difference for the carbon (liquid) fuel empire. But ICE was not the only cutting-edge technology: Bersanti and Matteucci built the first hydrogen engine in 1854, while Jenatzy managed to go beyond 100 km/h with an electric car in 1899. The reason for the supremacy of ICE over all the other technologies lies in two main factors: the first was the cost of production, the second was the weight/power ratio.

- Obviously, it was easy for factories to make and assemble just steel components, and the production lines were very efficient, lowering the costs. On the opposite side, electric motors were not so easy and cheap to produce, even because of the materials that were necessary to make batteries (this problem lasts even in our time).
- The weight/power ratio takes into account the weight of the propulsion system components (fuel, tank or batteries, engine or motor), and the power it can produce. The best choice is related even to the volume that it occupies.

So, as can be seen in figure 1.1 , to cover the same distance of 500 km, liquid fuel engine is much more compact than every other propulsion system.



Figure 1.1: liquid fuel systems volumes

Then, it has to be considered the power produced by the fuel, and, for the same mass, the results are shown in the figure 1.2 below.

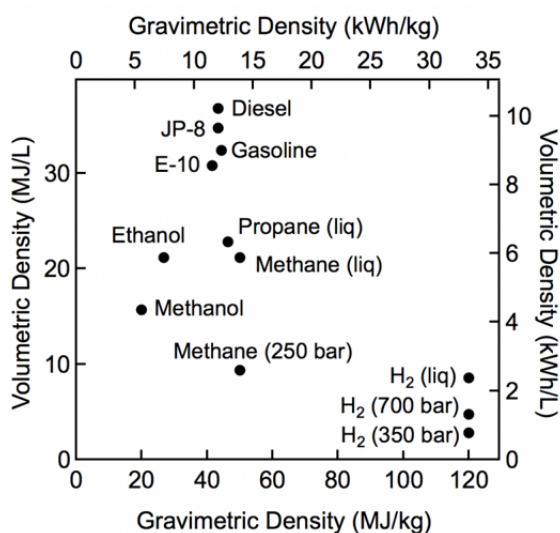


Figure 1.2: fuels gravimetric and volumetric density

The more the fuel is top right, the more power will produce; thus, to sum up, the liquid fuel propulsion system is the most compact one and the lighter one, and those characteristics made it the most used.

The more the fuel is top right, the more power will produce; thus, to sum up, the liquid fuel propulsion system is the most compact one and the lighter one, and those characteristics made it the most used.

- Otto engine works with gasoline and, because of the low reactivity of the fuel, it is necessary to have a spark to ignite the fuel-air gaseous mixture. The injection can be made either in the port (PFI) or the chamber (GDI). The injection system is represented in figure 1.3 (for the port fuel injection) and in figure 1.4 (for the gasoline direct injection).

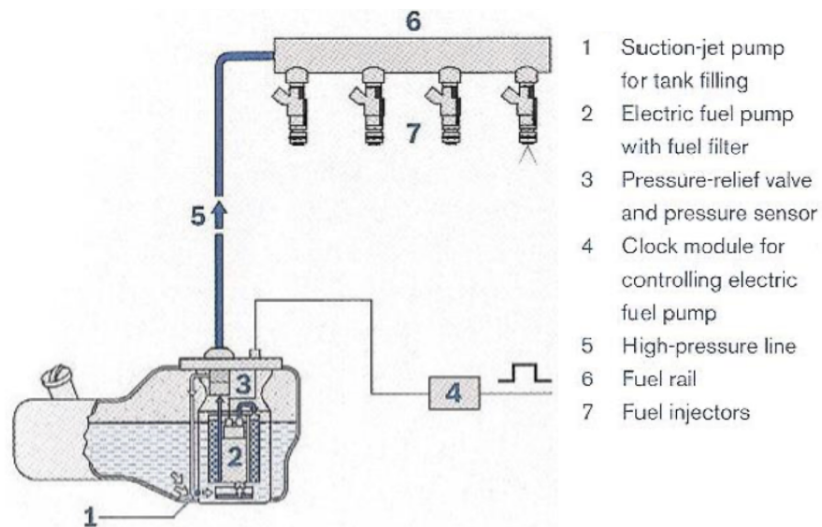


Figure 1.3: PFI injection system

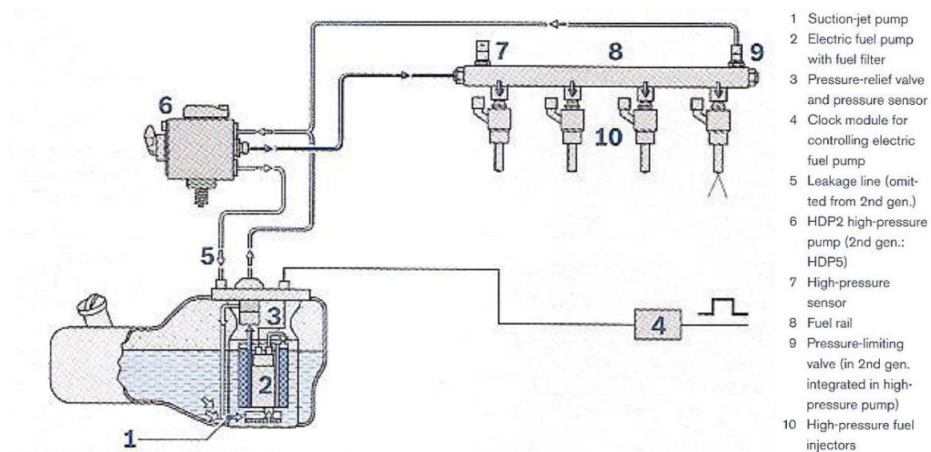


Figure 1.4: GDI injection system

It can be seen a pump, which is controlled by a signal from the ECU (electronic central unit) to be in sync with the injections. Fuel pressure depends on the technology: in PFI, fuel pressure is around 5 bar, because it has sufficient time to evaporate and start to create a mixture with air in the port, while in GDI fuel pressure is around 100 bar, because fuel is injected directly in the cylinder and has less time to evaporate (using a higher pressure is fundamental to maximize the velocity of the inlet liquid and thus its interaction with the air wall, causing the droplet to separate faster from the main jet).

To maintain the injection pressure constant and to have a more flexible system, a little high-pressure chamber has been developed, directly connected to injectors, called fuel common rail.

ECU commands injection timing using electric current: it can either charge a solenoid, whose electromagnetic field make the needle (inside the injector) move or actuate an electrovalve, or a piezoelectric actuator, which can be an element of a valve too, or directly connected to the main needle of the injector. Since the needle is totally inside its rise causes the injection, it is called inward opening.

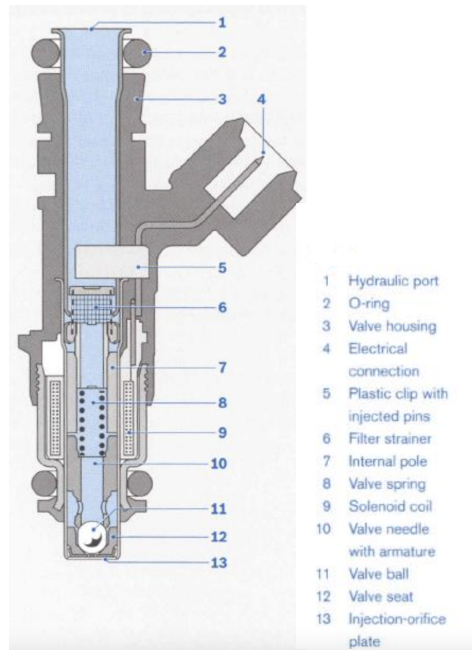


Figure 1.5: Gasoline injector

- Diesel engine works with oil and, because of its high reactivity, it is necessary to directly inject the fuel inside the chamber and, thanks to the high pressure and temperature inside the cylinder, the mixture will ignite by itself. The injection system is represented in figure 1.6

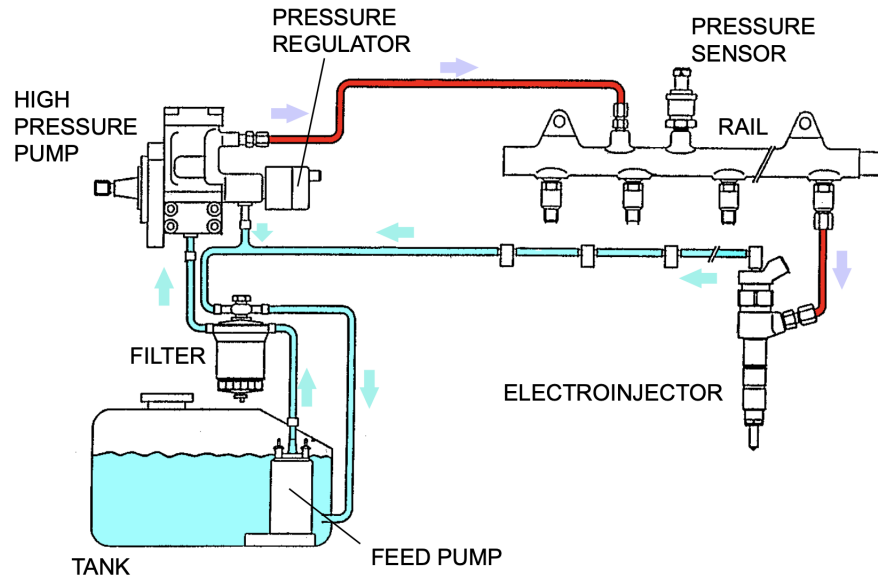


Figure 1.6: Diesel injection system

Control system is quite similar to the gasoline one, but here pressure is much higher. That's because fuel at sufficient conditions can fully react with air, so the injection, the evaporation and the combustion must happen in a short interval: thus the injection is directly inside the chamber at around 1000 bar pressure. The injector is shown in figure 1.7 (it is a solenoid-actuated model), inward as well.

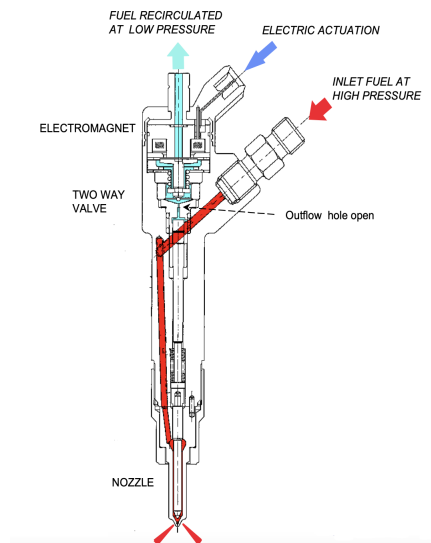
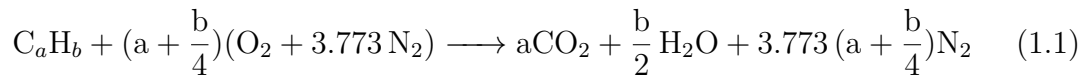


Figure 1.7: Diesel injector

To improve the combustion efficiency (just in Diesel engines) and to reduce the emissions (in both engines), may be useful to have more than one injection per cycle (up to 8). So modern systems can handle a higher injection frequency.

The main drawback of these technologies lies in their fuels: despite they are the most suitable for the cycle, they are a limited resource, moreover the combustion reaction of a reactant who contains carbon always leads to carbon dioxide.



In addition, the farther the effective combustion is from the ideal one, the more other pollutants are produced:

- NO_x , which originate at high temperature, since oxygen and nitrogen could not normally react.
- HC (unburnt hydrocarbons), which survives in the chamber, don't totally react and goes out from the engine.
- CO, that is a product of an incomplete combustion, since it not totally react to became CO_2 .
- PM (particulate matter), which forms at high temperature where a rich combustion happens (thus are typical of Diesel engines).

1.2 The decarbonization path

In the last decades, the environmental issue has become much more important, so a lot of countries started to regulate CO₂ emissions, since they are guilty of global warming. The first ambitious plan was the Kyoto protocol, signed in 1997 and entered into force in 2005, who required developed countries to limit their GHG (greenhouse gases) emissions in 2012, as compared to their emissions in 1990; moreover, it provides detailed methods and mechanisms for how the emission reductions can be achieved, measured and verified.

In 2009 a package known as 20-20-20 was adopted in Europe, which had the scope of reaching three targets by 2020: 20% reduction in EU greenhouse gas emissions from 1990 levels, 20% increase in the share of EU energy consumption produced from renewable resources, 20% improvement in the EU's energy efficiency.

In 2021 a new deal was submitted by UE: the "Fit for 55". It states that all countries must cut the CO₂ emissions by a certain date: for cars they must be reduced by 55% by 2030, while for trucks by 50%; then the goal is to reach zero emission (carbon neutrality) in 2035. Since many countries states that these aims are impossible to reach, the deal is currently under discussion.

For the pollutants, USA and Europe have chosen to face the problem in a different way, but they have in common the main idea that a vehicle (for trucks and off-road) or an engine (for passenger cars), to be sold, must pass an emission test; thus, if the considered pollutants emitted, in a proper driving cycle, are less than the limit, the vehicle or the engine will be homologated and it can be put on the market.

UE started to regulate the emissions in 1992, with the first limit called "Euro I"; in 2014 was adopted "Euro VI", that nowadays has become even stricter with the "Euro VI step D". In particular, there is a limit for every single pollutant. USA first pollutant regulation was made in 1994, called "Tier 1"; in 2014 was introduced the "Tier 4B" the strictest limits up to now. This law limits the sum of NO_x and NMOG (Non-Methane Organic Gas) emitted.

Despite the limits, automotive technology has improved very much to cut the pollutant emissions, giving birth to some very interesting devices:

- for gasoline engines, the 3-way catalyst (TWC) was introduced: it oxidates CO and HC and reduces NO_x. For the GDI, it is implemented a particulate filter too.
- for Diesel engines, three different technologies are coupled one after the other: DOC (Diesel oxidation catalyst) to oxidate HC and CO, SCR (selective catalytic reduction) to reduce NO_x and DPF (Diesel particulate filter) to block and oxidate the PM.

But for CO₂ emission, there is no aftertreatment system that can reduce it. It is produced naturally as a product of the combustion, so the only way to cut the

emissions is to improve the engine efficiency. That is the main reason why, in these years, another propulsion system has been demanded. Two possible solutions have been found: electric motors and hydrogen fuel. The main advantage of both technologies is that the vehicle CO₂ emissions (while it is driven, called also “tank to wheel”) is zero: the motor is totally electric, powered by the battery, while hydrogen reactions don’t produce carbon dioxide. Since gasoline and Diesel vehicles are still produced and sold, hydrogen could be the best alternative to face their possible ban, because a lot of technologies used for them could still be used even with another fuel, not revolutionizing the production lines.

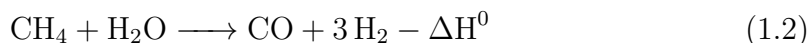
1.3 An alternative fuel: hydrogen

Hydrogen is the most abundant element in the universe. It is found as interstellar gas and as the chief constituent of main-sequence stars. On planets such as Earth, hydrogen is found as part of the molecules of water, methane, and organic material, whether fresh or fossilized. The normal molecular form is H₂[1]. Further properties are listed in the table 1.1 below.

Atomic number,H	1	
Molar mass, H ₂	2.016	10 ⁻³ kg mol ⁻¹
Ionic conductance of diluted H ⁺ in water at 298 K	0.035	m ² mol ⁻¹ Ω ⁻¹
Density, H ₂ at 101.33 kPa and 298 K	0.084	kg m ⁻³
Melting point at 101.33 kPa	13.8	K
Boiling point at 101.33 kPa	20.3	K
Heat capacity at constant pressure and 298K	14.3	kJ K ⁻¹ kg ⁻¹
Solubility in water at 101.33 kPa and 298 K	0.019	

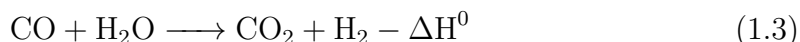
Table 1.1: Hydrogen properties[1]

Hydrogen production involves extracting and isolating hydrogen in the form of independent molecules, at the level of purity required for a given application[1]. Nowadays there are two main ways to do it: steam reforming or electrolysis. A lot of current industrial production of hydrogen starts from methane, CH₄, which is the main constituent of natural gas. A mixture of methane and water vapour (steam) at an elevated temperature (usually around 850°C) is undergoing the strongly endothermic reaction



where the enthalpy change ΔH^0 equals 252.3 kJ mol⁻¹ at ambient pressure (0.1 MPa) and temperature (298 K) and 206.2 kJ mol⁻¹ if the input water is already in

gas form. The carbon monoxide and hydrogen mixture on the right-hand side of the equation is called “synthesis gas”. This step requires a catalyst. The methane-steam ratio is not stoichiometric, because the excess of steam is useful to prevent cracking (and thus the possible coal formation) as well as CO excess[1]. In order to obtain a high conversion efficiency, some heat inputs are taken from cooling the reactants and from the heat outputs derived from the subsequent water-gas “shift reaction” (WGS reaction), usually taking place in a separate reactor:



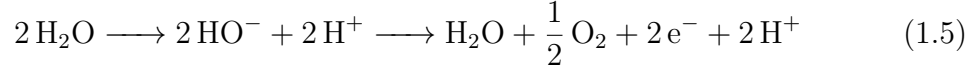
with ΔH^0 equal to -41.1 kJ/mol when all reactants are in gas form at ambient pressure and temperature and -5.0 kJ/mol if the water is liquid. Heat is recovered and recycled back to the first reaction 1.2. This involves two heat exchangers and is the main reason for the high cost of producing hydrogen by steam reforming. Industrial steam reformers typically use direct combustion of a fraction of the primary methane (although other heat sources could, of course, be used) to provide the heat required for the process:



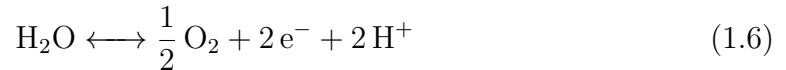
where $\Delta H^0 = -802.4$ kJ/mol for gaseous end products or -894.7 kJ/mol for liquid condensed water. This strategy to produce hydrogen is surely effective (with a theoretical efficiency of 100%, without considering the possible combustion reaction), but it creates oxygen dioxide as a product starting from methane (H_2 produced is called “blue hydrogen” if CO_2 is stored, while “grey hydrogen” if it is released in the atmosphere), so it is not a resolute technology to reach carbon neutrality[1].

The conversion of electric energy into hydrogen (and oxygen) by water electrolysis has been known for a long time (demonstrated by Faraday in 1820 and widely used since about 1890), but if the electricity is produced by the use of fossil fuels, then the cost of hydrogen obtained in this way is higher than the one associated with steam reforming of natural gas, furthermore it would be created anyway greenhouse gases. Thus, if the electricity used (to produce hydrogen) is a surplus from variable resources such as wind (that makes “green hydrogen”), solar radiation (that makes “yellow hydrogen”) this technique could become really interesting. In cases where such electricity is produced at times of no local demand and no evident option for export to other regions, the value of this electricity may be seen as zero. This makes it very favourable to store the energy for later use, and storage in the form of hydrogen is one option that may be very smart. That’s because electricity is doomed to deplete as time passes, while hydrogen is an excellent energy carrier and could be stocked and then used (even after time) in fuel cell reactors or burnt in engines[1]. So the combination of electrolysis and renewable energy sources

makes this technology very attractive. Conventional electrolysis uses an aqueous alkaline electrolyte, typically KOH, with the positive and negative electrode areas separated by a microporous membrane. The reaction at the positive electrode, where electrons are leaving the cell by way of the external circuit and where the three products may be formed by a two-step process, is



so the overall equation is



The reaction at the negative electrode is



Reaction 1.7 grabs electrons from the external circuit. The hydrogen ions are to be transported through the electrolyte by the electric potential difference. The role of the alkaline component is to improve on the poor ion conductivity of water. However, this limits process temperature to values below 100°C, in order to avoid strong increases in alkaline corrosion of electrodes. However, with the use of ambient heat at 25°C, the process would be very slow, so temperatures used in classical electrolyzers are around 80°C.

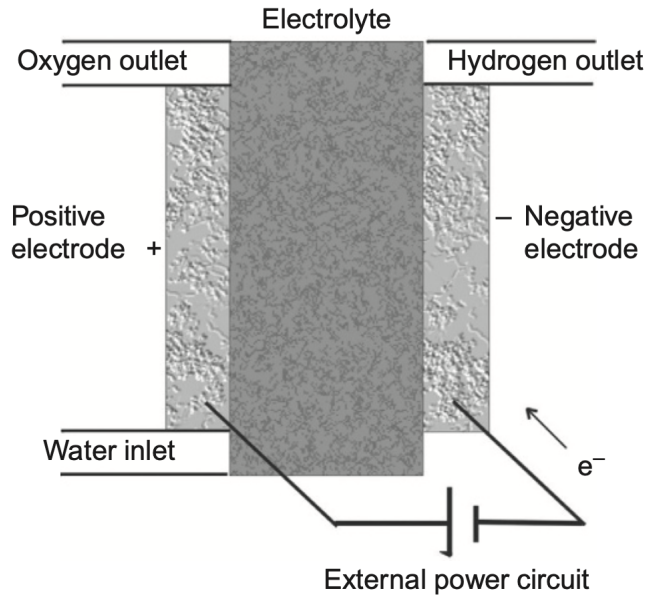
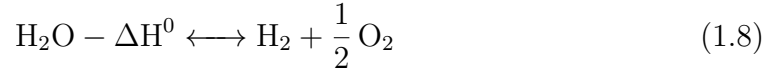


Figure 1.8: Bipolar plates[1]

Thus the overall reaction is the following



where ΔH^0 is -242 kJ/mol for gaseous steam and -288 kJ/mol for liquid water. Enthalpy formula is

$$\Delta H = \Delta G + T\Delta S \quad (1.9)$$

At ambient pressure and temperature (298 K), the change in enthalpy and free energy for liquid water is $\Delta H = -288$ kJ/mol and the free energy is $\Delta G = 236$ kJ/mol. The electrolysis process thus requires a minimum amount of electric energy of 236 kJ/mol. Since the apparent conversion efficiency would be $\frac{\Delta H}{\Delta G}$, it could theoretically exceed 100% by as much as 22%. The much lower conversion efficiency (50%–77%) obtained with simple electrolyzers in practical cases is largely a consequence of electrode “overvoltage”, mainly stemming from polarisation effects. The cell potential V for water electrolysis may be expressed by

$$V = V_r + V_a + V_c + R \cdot j \quad (1.10)$$

where V_r is the reversible cell potential, V_a and V_c are the resistance contribution of, respective, anode and cathode, while j is the current and R the internal resistance of the cell. Thus the three last terms in the equation 1.10 represent electrical losses, and the voltage efficiency η_V of an electrolyser [1] operating at a current j is defined by

$$\eta_V = \frac{V_r}{V} \quad (1.11)$$

After being produced, hydrogen becomes a very efficient and versatile energy carrier, that could be used to produce mechanical energy or electric energy. In automotive sector both paths are followed, respectively with internal combustion engines and fuel cells.

1.4 Hydrogen internal combustion engine

Hydrogen can be used as a fuel in conventional spark-ignition engines such as the Otto cycle one: as said before, this would be perfect to not revolutionize automotive production lines, making the radical abandonment of fossil fuels much smoother. Spark ignition engines are suitable for hydrogen but in recent times compression ignition engines are also in the process of modification to run with hydrogen. It is important to mention here that, since hydrogen has an auto-ignition temperature of about 576 °C, it is not possible to achieve its ignition by compression alone. Some

sources of ignition have to be created inside the combustion chamber to ensure ignition, such as the installation of glow plugs in the combustion chamber [2]. The injection is a crucial step for the correct operating of the engine, because if it is made in the wrong instant could cause a not wanted ignition: the low energy needed to ignite the hydrogen-air mixture promotes the occurrence of abnormal combustion events. The occurrence of mixture ignition is typically caused by contact with a hot surface or hot spots (residual gas or oil ash). While the intake valves are opened, this incidence is commonly known as back-firing. This phenomenon may generate the burn-up of the whole H_2 -air charge, generating a misfiring cycle and a knocking next cycle due to the intake heating [3]. With a port fuel injection (PFI) system, it is widely accepted that hydrogen injection timing is the most crucial parameter in avoiding back-firing. Suppose the injection starts too early, i.e., close to the intake valve opening (IVO) event, an ignitable mixture is formed in the intake port before the residual gas within the cylinder can be cooled by the air charge alone. On the other hand, if the injection ends too late, close to the intake valve closure (IVC), a considerable fraction of the injected fuel remains in the port. This remaining fuel mass forms an ignitable mixture on the next cycle and promotes a back-firing event at IVO [3]. In contrast, the direct injection (DI) method solely induces air during the intake stroke and injects hydrogen gas directly into the cylinder during the compression stroke. Fundamentally, because hydrogen gas does not exist in the intake pipe, backfire does not occur. In addition, as the intake air amount increases proportionally to the volume of hydrogen gas injected into the cylinder, the challenge of low output is also solved simultaneously. The in-cylinder direct injection method can be divided into early and late injections, depending on the injection timing of hydrogen gas. The early direct injection method injects hydrogen gas in the first half of the compression stroke, hence fuel with a relatively low pressure can be utilized [3]. To have a better control on injection, a pressure ratio, between the injector supply and the cylinder charge, should be kept above the critical one to ensure sonic conditions. Thus, the mass flow rate is not dependent on the conditions downstream of the injector nozzle, and precise injections can be obtained throughout the whole engine operational map [3]. Fuel pressure could vary a lot from strategy to strategy (from 15 bar to 500 bar), even if it seems that low pressure injection is more convenient: a large amount of the hydrogen gas, 20% in the case of the injection pressure of 10 MPa, and 37% in the case of the injection pressure of 20 MPa, becomes inaccessible as the tank is emptied. This is due to the pressure in the container becoming lower than the required injection pressure. This greatly reduces the effective driving range [4]. But obviously a less pressurized gas requires more volume to have a sufficient driving range. Liquid hydrogen resolves this problem: as seen before, liquid fuels are superior to the gaseous one in terms of volume/power ratio; furthermore liquid, when injected in the chamber, evaporate and cools down all other gases. The drawback is that hydrogen boiling temperature

is around 20 K (as reported in table 1.1), so it is very difficult to apply this idea outside a laboratory. Hydrogen injectors are quite similar to the gasoline one, they can be opened by charging a solenoid or a piezoelectric stack and closed by a preloaded spring.

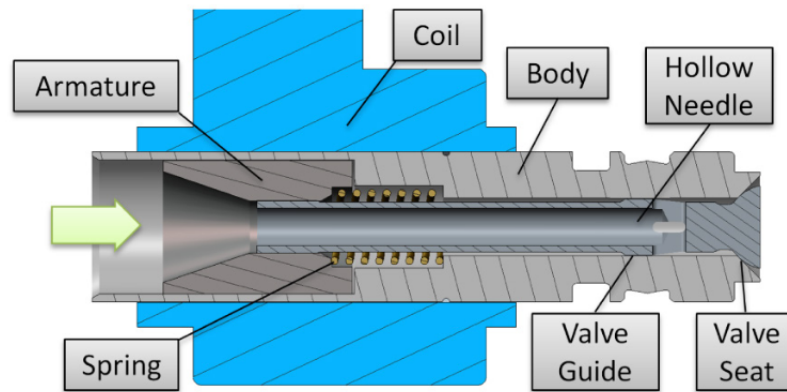


Figure 1.9: Hydrogen outward injector[5]

Hydrogen injectors could have a different layout depending on the direction of needle lift: outward opening or inward opening.

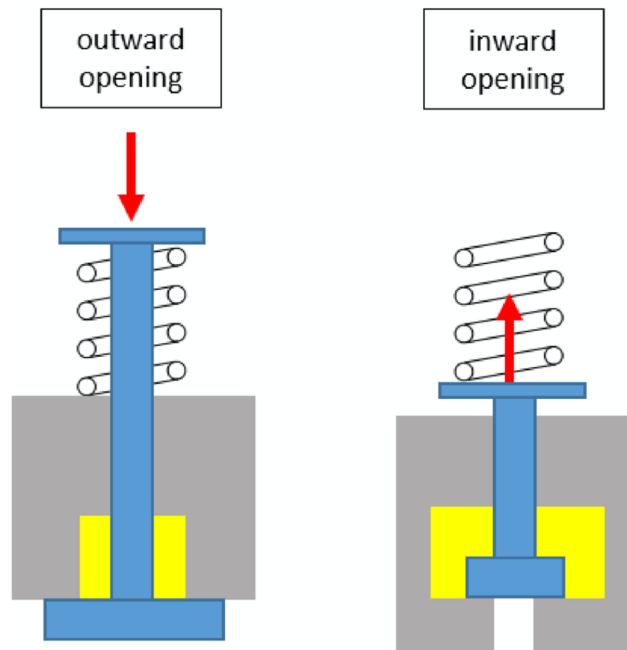


Figure 1.10: Outward and inward hydrogen injector[3]

In both design principles, a closing spring applies a force on the sealing contact area to keep the injector closed. An actuation force (red arrow) must be applied to open the injector. In the outward opening injector, the combustion pressure supports the sealing (self-sealing effect). In the inward opening injector, the closing spring must be strong enough to prevent undesired opening. For LP-DI (low pressure direct injection), the firing pressure is far greater than the H₂ supply pressure (present in the volume marked in yellow). Hence, the inward opening injector requires a much stronger closing spring than the outward opening injector, and consequently, a greater force is needed to open the injector. During those phases where the cylinder pressure is lower than the H₂ supply pressure (for example during the suction stroke and the early phase of compression), the inward opening injector benefits from a self-sealing effect since the pressure difference acts now in the closing direction. In case of a failure of the closing spring, no hydrogen can escape uncontrolled into the combustion chamber [3].

Since, inside the chamber, combustion occurs, NO_x will be produced. As happens in ICE, there are some strategy that could be use inside the engine and outside it to lower pollutants quantity:

- early injection is the best under low- speed, low-load conditions, as it maintains 35% BTE while keeping NO_x at approximately zero [3].
- with multiple injection strategies it was found that when the secondary injection accounts for 50%, the NO_x emission is reduced by 85% compared to the single injection [3].
- exhaust gas recirculation (EGR) is also regarded as an effective measure to increase the polytropic index and reduce the combustion temperature [3].
- SCR technology is used to reduce NO_x in an aftertreatment system, as happens in Diesel engines.

1.5 Hydrogen fuel cell

A fuel cell can be seen as a “factory” that takes fuel as input and produces electricity as output. Like a factory, a fuel cell will continue to churn out product (electricity) as long as raw material (fuel) is supplied. This is the key difference between a fuel cell and a battery. While both rely on electrochemistry to work, a fuel cell is not consumed when it produces electricity. It is really a factory, which transforms the chemical energy stored in a fuel into electrical energy [6].

The main difference between how ICE and fuel cell generates energy lies in the way the hydrogen oxidation reaction 1.12 takes place.





Figure 1.11: Fuel cell reactants and products[6]

In engines, collisions between hydrogen molecules and oxygen molecules result in a reaction. The hydrogen molecules are oxidized, producing water and releasing heat. Specifically, at the atomic scale, in a matter of picoseconds, hydrogen–hydrogen bonds and oxygen–oxygen bonds are broken, while hydrogen–oxygen bonds are formed. These bonds are broken and formed by the transfer of electrons between the molecules. The energy of the product water bonding configuration is lower than the bonding configurations of the initial hydrogen and oxygen gases. This energy difference is released as heat. Although the energy difference between the initial and final states occurs by a reconfiguration of electrons as they move from one bonding state to another, this energy is recoverable only as heat because the bonding reconfiguration occurs in picoseconds at an intimate, subatomic scale [6].

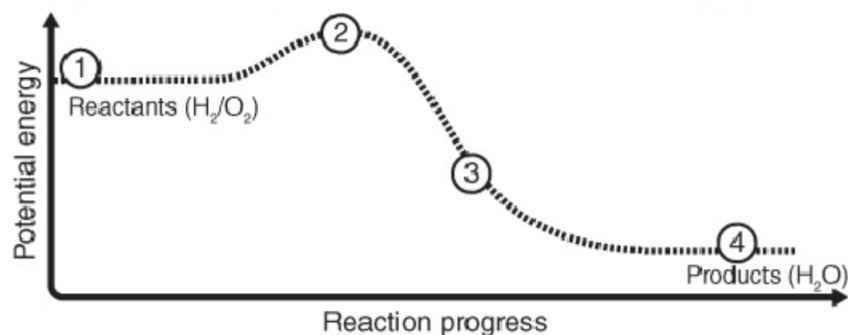


Figure 1.12: Energy of reactants and products of a fuel cell[6]

Electricity could anyway be directly produced from the chemical reaction by somehow harnessing the electrons as they move from high-energy reactant bonds to low-energy product bonds. This result could be reached spatially separating the hydrogen and oxygen reactants so that the electron transfer, necessary to complete the bonding reconfiguration, occurs over a greatly extended length scale. Then, as the electrons move from the fuel species to the oxidant species, they can be harnessed as an electrical current. The reactions that happen here are the reverse of the 1.6 and 1.7 so free electrons and ions are formed in the two electrodes. By

spatially separating these reactions, the electrons transferred from the fuel are forced to flow through an external circuit (thus constituting an electric current) and do useful work before they can complete the reaction. Spatial separation is accomplished by employing an electrolyte. An electrolyte is a material that allows ions (charged atoms) to flow but not electrons. At a minimum, a fuel cell must possess two electrodes, where the two electrochemical half reactions occur, separated by an electrolyte [6].

There are more types of fuel cells, depending of the electrolyte material:

- Phosphoric acid fuel cell (PAFC)
- Polymer electrolyte membrane fuel cell (PEMFC)
- Alkaline fuel cell (AFC)
- Molten carbonate fuel cell (MCFC)
- Solid-oxide fuel cell (SOFC)

While all five fuel cell types are based on the same underlying electrochemical principles, they all operate at different temperature regimens, incorporate different materials, and often differ in their fuel tolerance and performance characteristics. PEMFC is one of the most used, because it operates at low temperature (about 80°C) and have high power density; PEMFCs employ a thin polymer membrane as an electrolyte (the membrane looks and feels a lot like plastic wrap). The most common electrolyte is a membrane material called Nafion. Protons are the ionic charge carrier in a PEMFC membrane. Platinum is the catalyst. The half reactions are mediated by the movement of protons (H^+) and water is produced at the cathode.

The current (electricity) produced by a fuel cell scales with the size of the reaction area where the reactants, the electrode, and the electrolyte meet. In other words, doubling a fuel cell's area approximately doubles the amount of current produced. Although this trend seems intuitive, the explanation comes from a deeper understanding of the fundamental principles involved in the electrochemical generation of electricity. As we have discussed, fuel cells produce electricity by converting a primary energy source (a fuel) into a flow of electrons. This conversion necessarily involves an energy transfer step, where the energy from the fuel source is passed along to the electrons constituting the electric current. This transfer has a finite rate and must occur at an interface or reaction surface. Thus, the amount of electricity produced scales with the amount of reaction surface area or interfacial area available for the energy transfer. Larger surface areas translate into larger currents. To provide large reaction surfaces that maximize surface-to-volume ratios, fuel cells are usually made into thin, planar structures. The electrodes have

an highly porous layer called GDL (gas diffusion layer) to further increase the reaction surface area and ensure good gas access. One side of the planar structure is provisioned with fuel (the anode electrode), while the other side is provisioned with oxidant (the cathode electrode). A thin electrolyte layer spatially separates the fuel and oxidant electrodes and ensures that the two individual half reactions occur in isolation from one another [6]. Fuel cells work when four steps are successfully completed:

1. Reactant transport: for a fuel cell to produce electricity, it must be continually supplied with fuel and oxidant. This seemingly simple task can be quite complicated. When a fuel cell is operated at high current, its demand for reactants is voracious. If the reactants are not supplied to the fuel cell quickly enough, the device will “starve.” Efficient delivery of reactants is most effectively accomplished by using flow field plates in combination with porous electrode structures. Flow field plates contain many fine channels or grooves to carry the gas flow and distribute it over the surface of the fuel cell [6].
2. Electrochemical reaction: once the reactants are delivered to the electrodes, they must undergo electrochemical reaction. The current generated by the fuel cell is directly related to how fast the electrochemical reactions proceed. Fast electrochemical reactions result in a high current output from the fuel cell. Sluggish reactions result in low current output. Obviously, high current output is desirable. Therefore, catalysts are generally used to increase the speed and efficiency of the electrochemical reactions. Fuel cell performance critically depends on choosing the right catalyst and carefully designing the reaction zones. Often, the kinetics of the electrochemical reactions represent the single greatest limitation to fuel cell performance [6].
3. Ionic (and electronic) conduction: the electrochemical reactions occurring in step 2 either produce or consume ions and electrons. Ions produced at one electrode must be consumed at the other electrode. The same holds for electrons. To maintain charge balance, these ions and electrons must therefore be transported from the locations where they are generated to the locations where they are consumed. For electrons this transport process is rather easy. As long as an electrically conductive path exists, the electrons will be able to flow from one electrode to the other. In a simple fuel cell, for example, a wire provides a path for electrons between the two electrodes. For ions, however, transport tends to be more difficult. Fundamentally, this is because ions are much larger and more massive than electrons. An electrolyte must be used to provide a pathway for the ions to flow. In many electrolytes, ions move via “hopping” mechanisms. Compared to electron transport, this process is far less efficient. Therefore, ionic transport can represent a significant resistance

loss, reducing fuel cell performance. To combat this effect, the electrolytes in technological fuel cells are made as thin as possible to minimize the distance over which ionic conduction must occur [6].

4. Product removal: in addition to electricity, all fuel cell reactions will generate at least one product species. The H_2-O_2 fuel cell generates water. Hydrocarbon fuel cells will typically generate water and carbon dioxide. If these products are not removed from the fuel cell, they will build up over time and eventually “strangle” the fuel cell, preventing new fuel and oxidant from being able to react. Fortunately, the act of delivering reactants into the fuel cell often assists the removal of product species out of the fuel cell. The same mass transport, diffusion, and fluid mechanics issues that are important in optimizing reactant delivery (step 1) can be applied to product removal. Often, product removal is not a significant problem and is frequently overlooked. However, for certain fuel cells (e.g., PEMFC) “flooding” byproduct water can be a major issue [6].

The performance of a fuel cell device can be summarized with a graph of its current–voltage characteristics. This graph, called a current–voltage (i-V) curve, shows the voltage output of the fuel cell for a given current output. An example of a typical curve for a PEMFC is shown in figure 1.13. Note that the current has been normalized by the area of the fuel cell, giving a current density (in amperes per square centimeter). Because a larger fuel cell can produce more electricity than a smaller fuel cell, i-V curves are normalized by fuel cell area to make results comparable. An ideal fuel cell would supply any amount of current (as long as it is

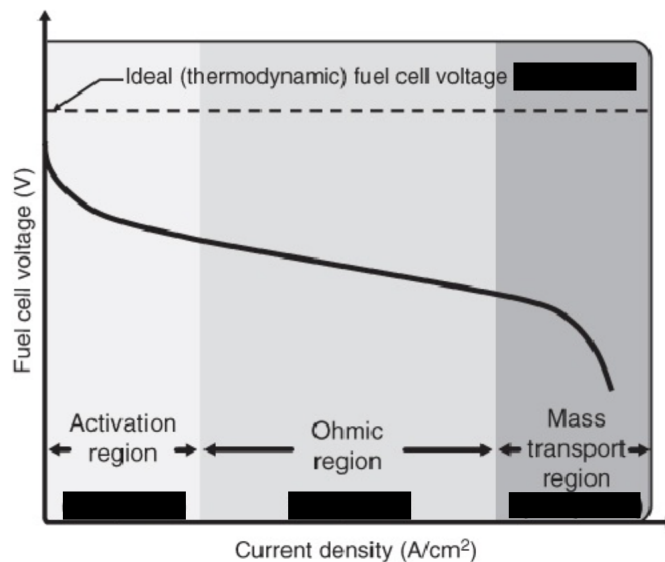


Figure 1.13: Fuel cell voltage losses[6]

supplied with sufficient fuel), while maintaining a constant voltage determined by thermodynamics. In practice, however, the actual voltage output of a real fuel cell is less than the ideal thermodynamically predicted voltage. Furthermore, the more current that is drawn from a real fuel cell, the lower the voltage output of the cell, limiting the total power that can be delivered. The power P delivered by a fuel cell is given by the product of current and voltage:

$$P = V \cdot i \quad (1.13)$$

A fuel cell power density curve, which gives the power density delivered by a fuel cell as a function of the current density, can be constructed from the information in a fuel cell i - V curve. The power density curve is produced by multiplying the voltage at each point on the i - V curve by the corresponding current density. The current

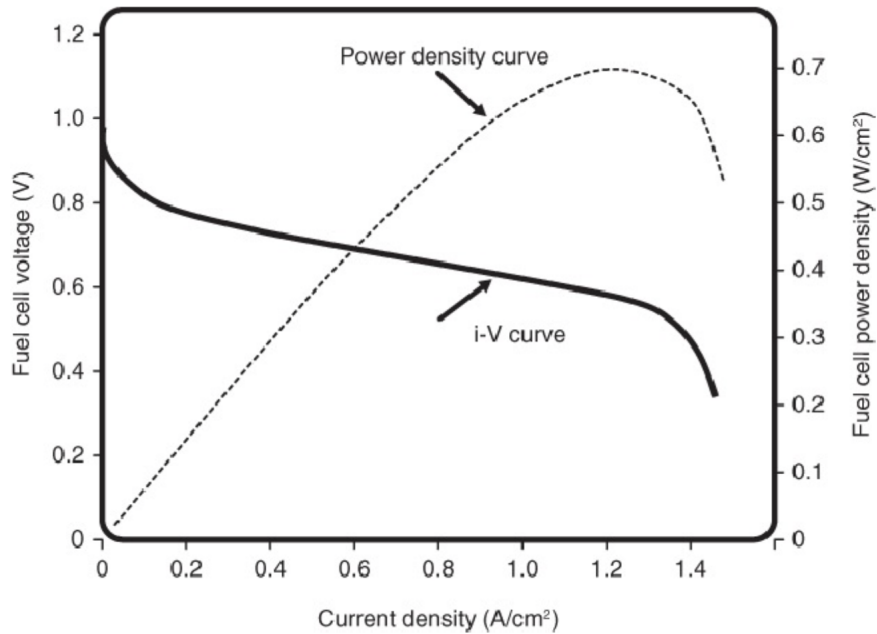


Figure 1.14: Fuel cell operating curve[6]

supplied by a fuel cell is directly proportional to the amount of fuel consumed (each mole of fuel provides two moles of electrons). Therefore, as fuel cell voltage decreases, the electric power produced per unit of fuel also decreases. In this way, fuel cell voltage can be seen as a measure of fuel cell efficiency. Maintaining high fuel cell voltage, even under high current loads, is therefore critical to the successful implementation of the technology. Unfortunately, it is hard to maintain a high fuel cell voltage under the current load. The voltage output of a real fuel cell is less than the thermodynamically predicted voltage output due to irreversible

losses. The more current that is drawn from the cell, the greater these losses. There are three major types of fuel cell losses, which give a fuel cell i–V curve its characteristic shape. Each of these losses is associated with one of the basic fuel cell steps discussed before:

1. Activation losses (losses due to electrochemical reaction)
2. Ohmic losses (losses due to ionic and electronic conduction)
3. Concentration losses (losses due to mass transport)

The real voltage output for a fuel cell can thus be written by starting with the thermodynamically predicted voltage output of the fuel cell and then subtracting the voltage drops due to the various losses:

$$V = E_{thermo} - \eta_{act} - \eta_{ohmic} - \eta_{conc} \quad (1.14)$$

where V is the real output voltage of fuel cell, E_{thermo} is thermodynamically predicted fuel cell voltage output, η_{act} is activation losses due to reaction kinetics, η_{ohmic} is ohmic losses from ionic and electronic conduction, while η_{conc} represents concentration losses due to mass transport. The three major losses each contribute to the characteristic shape of the fuel cell curve. As shown in Figure 1.13, the activation losses mostly affect the initial part of the curve, the ohmic losses are most apparent in the middle section of the curve, and the concentration losses are most significant in the tail of the curve.

While studying fuel cell, an important constant that usually appears is the term nF ; this quantity is the bridge from the world of thermodynamics (where moles of chemical species are used) to the world of electrochemistry (where current and voltage are used). In fact, the quantity nF expresses one of the most fundamental aspects of electrochemistry: the quantized transfer of electrons, in the form of an electrical current, between reacting chemical species. In any electrochemical reaction, there exists an integer correspondence between the moles of chemical species reacting and the moles of electrons transferred. For example, in the fuel cell reaction 1.7, 2 mol of electrons is transferred for every mole of H_2 gas reacted. In this case, $n=2$. To convert this molar quantity of electrons to a quantity of charge, we must multiply n by Avogadro's number N_A to get the number of electrons and then multiply by the charge per electron q to get the total charge. Thus we have

$$Q = n \cdot N_A \cdot q = n \cdot F \quad (1.15)$$

Thus the Faraday constant's value is

$$F = N_A \cdot q = (6,022 \cdot 10^{23} \text{ electrons/mol}) \cdot (1,6 \cdot 10^{-19} \text{ C/electron}) = 96485 \text{ C/mol} \quad (1.16)$$

It could be noticed that just a little quantity of electrons produce a lot of electricity: these is one of the main advantages of fuel cells. Furthermore, this simple relationship between the electrons produced and the molecules consumed is very useful to design an efficient control system. Because fuel cells are “factories” that produce electricity as long as they are supplied with fuel, they share some characteristics in common with combustion engines. Because fuel cells are electrochemical energy conversion devices that rely on electrochemistry to work, they share some characteristics in common with primary batteries. In fact, fuel cells combine many of the advantages of both engines and batteries. Since fuel cells produce electricity directly from chemical energy, they are often far more efficient than combustion engines. Fuel cells can be all solid state and mechanically ideal, meaning no moving parts. This yields the potential for highly reliable and long-lasting systems. A lack of moving parts also means that fuel cells are silent. Also, undesirable products such as NO_x , SO_x , and particulate emissions are virtually zero. Unlike batteries, fuel cells allow easy independent scaling between power (determined by the fuel cell size) and capacity (determined by the fuel reservoir size). In batteries, power and capacity are often convoluted. Batteries scale poorly at large sizes, whereas fuel cells scale well from the 1 W range (cell phone) to the megawatt range (power plant). Fuel cells offer potentially higher energy densities than batteries and can be quickly recharged by refueling, whereas batteries must be thrown away or plugged in for a time-consuming recharge [6]. While fuel cells present intriguing advantages, they also possess some serious disadvantages. Cost represents a major barrier to fuel cell implementation. Because of prohibitive costs, fuel cell technology is currently only economically competitive in a few highly specialized applications (e.g., onboard the Space Shuttle orbiter). Power density is another significant limitation. Power density expresses how much power a fuel cell can produce per unit volume (volumetric power density) or per unit mass (gravimetric power density). Although fuel cell power densities have improved dramatically over the past decades, further improvements are required if fuel cells are to compete in portable and automotive applications. Combustion engines and batteries generally outperform fuel cells on a volumetric power density basis; on a gravimetric power density basis, the race is much closer [6].

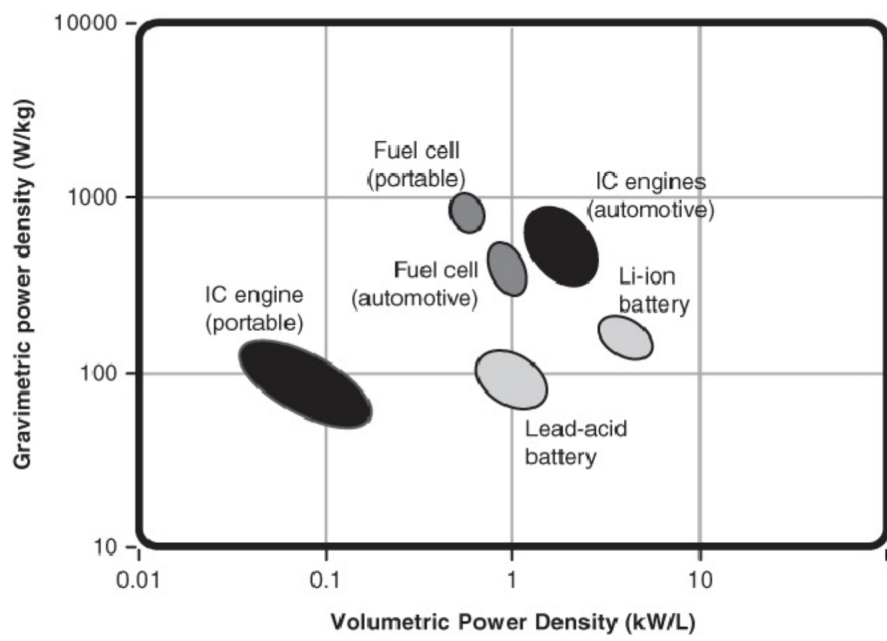


Figure 1.15: Comparison between engines and fuel cells[6]

Chapter 2

The Monaco energy boat challenge

The Monaco Energy Boat Challenge is a competition, owned and managed by the Yacht Club de Monaco, whose goal is to aim to a future propulsion technology. A cutting-edge energy source could be implemented in the boat, like electricity, hydrogen and sun. As a matter of fact, three categories of propulsion systems are admitted, each separated from the others:

- Open sea class, in which may participate fossil fuel boats
- Solar class, in which may participate boats whose main energy source is sun
- Energy class, in which may participate boats with other (tank to wheel) carbon free energy source, like hydrogen, sun, electricity (stocked inside a battery).

For every propulsion strategy there are a different rules. This work aims to model a hydrogen fuel cell boat, thus competing in the energy class.

2.1 Energy class rules

Since, in the energy class [7], various energy source are allowed, even in the same boat, the maximum amount of energy inside the vehicle is imposed, which is 10 kWh. To make the competition more fair, the organisers set a parameter, called energy factor f_i , that should counterbalance the efficiency of the energy source to produce electricity. For example the energy factor value is 0.4 for hydrogen and 1 for batteries. To sum up, the total energy that could be stocked inside the boat E_{tot} is 10 kWh, and it is equal to the sum of all the energy sources E_i multiplied for the respective energy factor:

$$E_{tot} = \sum f_i \cdot E_i \quad (2.1)$$

An other rule that is fundamental for the model is the maximum hydrogen relative pressure, which is 700 bar. Thus, the energy equation 2.1 opens a lot of possibilities, building even a hybrid power supply, as for example a fuel cell and a battery connected in parallel to an electric motor.

The Yacht Club de Monaco put at the disposal of each selected team a hull: it is made by two hulls and two beams bolted together in a catamaran shape. The beams are round carbon fibre poles. They will be used to support and secure the cockpit. The overall dimensions is reported in table 4.3

Overall length	5 m
Overall width	2.5 m
Free board hight	0.45 m
Beam diameter	10.4 cm
Longitudinal distance between beams	3 m
Total weight of hulls + beams	60 kg

Table 2.1: Boat main dimensions[7]

Before the race, inspector verify that the all the rules are respected, than they proceed to verify the boat controllability, the racing skills of the pilot and the freeboard in racing condition. If it passes all these tests, it is allowed to take part to the competitions. For the energy class the main events are:

- The maneuverability test, in which the ability of the boat to move efficiently in the Monaco harbour. This trial will be explained in a more detailed way in chapter 5.1
- The speed record trial, where, for 1 km straight, the boat speed is measured. It was not considered important for the boat design in this work, since the endurance was a priority. The path is indicated in figure 2.1



Figure 2.1: Speed trial course[8]

- The endurance trial, in which is tested that the boat can move no stop for 4 hours in a circular circuit 1 nautical mile long. The goal of the teams is to complete more laps; it is important to notice that laps are counted even if the boat stops because of a lack of fuel even before the 4 hours. The race course, and the design of the powertrain to run it, is explained in chapter 5.2
- The actual race, made by a single lap of the endurance race course (nautical mile long); in chapter 5.3 a full power cycle is simulated; it has to be stated that the endurance race gives double points that the one lap, with the same ranking.

Chapter 3

The fuel cell model

3.1 The software Simcenter Amesim

To create the model of the entire boat the software Simcenter Amesim [9] was used. It is a system simulation platform that allows design engineers to virtually assess and optimize the systems. It is a leading integrated, scalable system simulation platform, allowing system simulation engineers to virtually assess and optimize the performance of mechatronic systems. Simcenter Amesim combines ready-to-use multiphysics libraries with the application and industry-oriented solutions that are supported by powerful platform capabilities. Simcenter Amesim is an open environment that can be integrated into enterprise processes. Users can easily couple it with major computer-aided engineering (CAE), computer-aided design (CAD) and control software packages, interoperate it with the Functional Mockup Interfaces (FMIs), and connect it with other Simcenter solutions and Teamcenter software. Simcenter Amesim is part of the Siemens Xcelerator portfolio, the comprehensive and integrated portfolio of software and services from Siemens Digital Industries Software.

The convenience of this program lies in the fact that multiphysical models could be coupled together. This really simplifies the design and simulation of all boats components. In the model of the boat more libraries have been used, each identified even graphically with a different colour:

- the gas mixture library, to simulate the air and hydrogen supply systems and the respective outlet pipes
- the fuel cell library, to model the fuel cell stack component and the hydrogen tank
- the thermal library to model the cooling system of the stack

- the electric library, to model the electrical circuits and the electrical motors
- the 1D dynamic library to simulate the gears and shaft of the electric powertrain
- the aircraft and marine library to model the propeller of the boat and the hull resistance
- the signal library, to model the control strategies for the accessory systems of the fuel cell.

The first goal to reach is to successfully model the fuel cell. It is based on a real one the DEA 1.0 [10], made by MES company. The main fuel cell is made of several subcomponents which, in the following chapters, will be separately described.

3.2 Gases and materials definitions

The first thing to be set are the gases and materials that will be used in the whole model. The gases, that are used here, are inserted using the "generic gas definition" component, that allows to include in the model a gaseous molecule, present in the Amesim database. Five gases are defined: O₂, N₂, H₂, H₂O and CO₂. Then, since at anode and cathode, the percentages of these gases are different, two different mixtures are created, using the "gas mixture definition" components. The correct percentage are set in every component of the "gas mixture" library, as pipe and chamber. Moreover water needs an other specific definition, because it can condensate: so two more components are added to import in the model the water properties, the "moist air condensate definition" and the "thermal-hydraulic water" components; all the physical and thermal characteristics of water are already stored inside Amesim database. Then two solid materials are defined:

- the GDL (that will be explained in chapters 3.4 and 3.5) material, using the "thermal solid properties" component, setting a density of 325.58 kg/m³, a specific heat of 1000 J/(kg · K) and a thermal conductivity of 0.3 1000 W/(m · K) [11];
- the steel in which the whole fuel cell stack is made, AISI 316 [10]. It is inserted in the model with the "thermal solid properties" component again, but this time its properties are already stored inside Amesim database.

The last two elements to be inserted are necessary for the radiator and the coolant system:

- the "define ambient temperature and pressure component", useful for imposing the properties of the radiator cooling air.

- the "thermal-hydraulic fluid properties", that is necessary to define the characteristics of the coolant; a mixture of 50% water and 50% glycol, whose properties are already saved inside the Amesim database, specifying not to consider cavitation and aeration in this model.



Figure 3.1: Materials, gases and liquids definition

3.3 Fuel cell stack model

The heart of the whole model and the whole project is the fuel cell. All its auxiliaries (air supply system, hydrogen supply system, cooling system and control system) are described in the next chapters. Amesim already has, in the fuel cell library, the stand-alone "fuel cell stack" component, that only needs some setting parameters to start to work. All of them have been read from a manual of a MES fuel cell [10], not an open cathode, but at least useful to complete a preliminary model.

In the manual, different fuel cell ratings are presented; the rated power of 1.5 kW was chosen (the reason will be explained in the chapter related to the boat propulsion system). The main characteristics of the stack are:

Nominal Power	1500	W
Stack Voltage Range	36-57	V
Nominal Stack Voltage	36	V
Nominal Stack Current	45	A
Number of cells	60	
Active Area	61	cm ²
Stack weight	4.05	kg
External Supply Voltage	12	V

Table 3.1: Fuel cell datasheet [10]

To reach the voltage and current operating range, the cell voltage parameter was set to 0.7 V, while the global voltage computation was set to be calculated by

equations (already tuned in Amesim), using the boundary condition of the model, like pressure, concentration and temperature of the gaseous molecules or the stack temperature. The weight of the 1.5 kW stack was calculated, making a proportion with the weight of the 1 kW one, which was 2.7 kg; furthermore, it had 40 cells (1.5 times less than the 1 kW one).

The fuel cell component allows to include the physical properties of the bipolar plates: the membrane water transport (diffusion and electro-osmosis) and the O₂, N₂, H₂ membrane diffusion was set. The polarization curve is the following in figure 3.2:

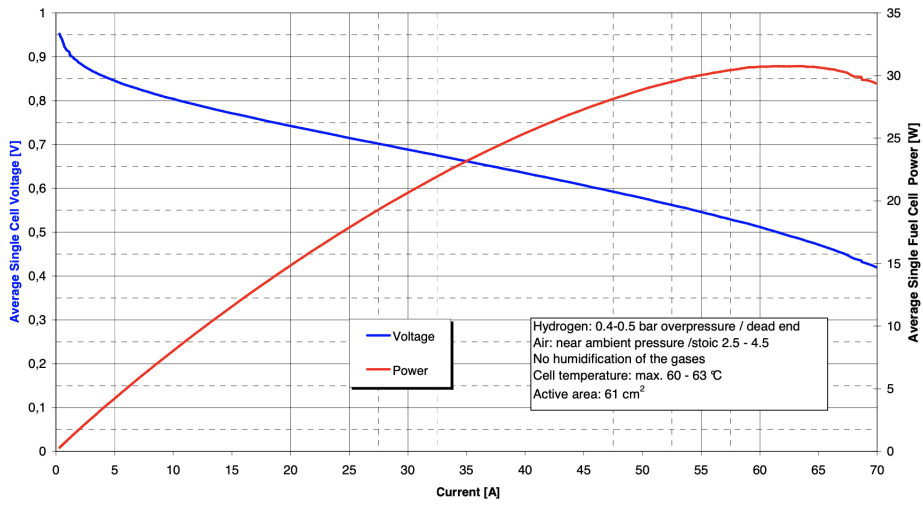


Figure 3.2: Polarization curve [10]

Then the gas mixture has to be defined in the fuel cell component too: at the cathode, since ambient air is flowing, the percentages are, respectively, 21%, 78%, 0%, 0% and 1%, while at the anode side there is 100% hydrogen, at the beginning of the simulation.

The fuel cell component is connected to the "thermal capacity component", which simulates the thermal behaviour of the stack: it is made of AISI 316 steel, whose properties are already integrated inside the Amesim database; its temperature is imposed to the working condition, which is 60°C. This component has two other ports, that are connected, through the "external mixed convective exchange with thermal port" component, to the anode and cathode chamber, representing the convective heat exchange between the electrodes and the gases. Thus the exchange area is the total area of the electrodes.

3.4 Air supply system

The first submodel, to be analysed, is the air supply system, which is sketched, with its main components, in figure 3.3 and modelled in figure 3.4.

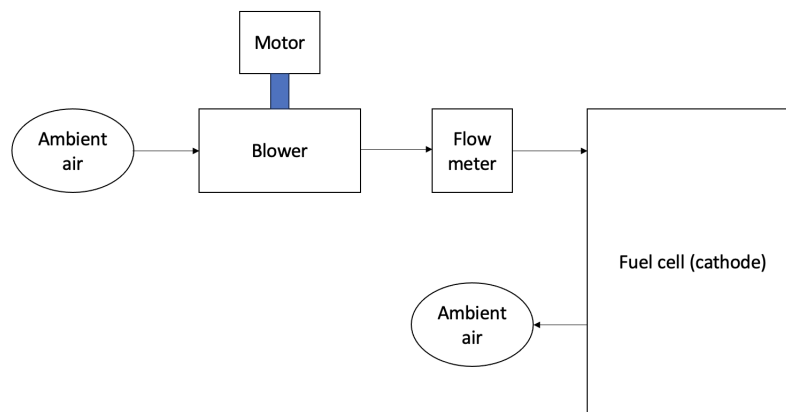


Figure 3.3: Oxygen supply system scheme

As described in chapter 1, the reaction of fuel cells involves oxygen and hydrogen: oxygen is directly taken from the ambient air. It is important to say that, since the fuel cell is an open cathode one (the reason why is explained later in this chapter), the coolant system and the air supply system are strictly connected: the blower used to cool the radiator pipe is the same that must deliver enough oxygen to the cathode electrode. For this reason, this fan has the highest power demand of all the auxiliary systems. Furthermore, the fuel cell is mounted on a boat, so the movement of the boat causes a certain inlet air speed on its own, even without the fan rotating.

- So the first component to be modelled is the "conversion of a signal into an air velocity and ambient temperature source". The input signal is the boat velocity. The ambient temperature is set using the "define ambient temperature and pressure" component, explained in chapter 3.2.
- the second component to be inserted is the "radiator and fan with air velocity imposed by port 1": the input at port 1 in the output of the component defined just above, while the radiator characteristics are set (they will be explained in a detailed way in chapter 3.6); for the air supply system the interesting parameters to be set are the one of the fan [12] (the OD254AP-12H*BIP68 was chosen, with an absorbed power of 65 kW); an other input to this component is the activation signal: it can varies from 0 (off) to 1 (on at nominal speed) and it is set by the control system, to guarantee both the coolant refrigeration

and the oxygen supply to the electrodes. The main output are two signals, that represents the outlet air temperature and flow rate from the radiator (basically this signals simulates a flowmeter output, already included in the radiator component).

- the next component is the "moist air modulated temperature, mass flow rate and humidity source"; it generates a moist air flow rate, that will enter in the fuel cell chamber. It needs four input: the air temperature, the mass flow rate (these two are directly taken from the radiator output, just correcting the unit of measurements), the relative humidity (seen in the weather forecast) and the dry air composition (this one is a multiplexed signal, made by four other signals, with the percentage of each molecule: O₂, N₂, CO₂, H₂ and H₂O, in the respective percentage of 21%, 77%, 1%, 0% and 1%).
- the next component is the fuel cell cathode chamber, with a volume of 2 L, modelled using the "gas mixture chamber with heat exchange"; it has three ports, one for the air inlet, one connected to the fuel cell stack and the other one for the air outlet to the ambient.
- the cathode chamber is connected with the "gas mixture porous media with diffusion" component, that simulates the GDL (Gas Diffusion Layer); it slows down the air close to the electrodes. It is made by a material called SIGRACET, made by SGL Carbon GmbH [11]. It has a thickness of 1 mm, a surface of 3660 cm² (calculated multiplying the cell active area per the cells numbers), a permeability of $2.8 \cdot 10^{-12}$ m² and a porosity of 0.82.
- just after that, a little chamber of 0.5 L is modelled, using the "gas mixture chamber without heat exchange" component, to simulate the space between the electrode and the GDL.
- the air outlet pipe is modelled, using the "gas mixture pipe with friction (R) and optional inertia (IR)"; since there is no pipe in the reality, but the fuel cell cathode channels are directly connected to the open air, the diameter of this component is set to 192 mm (as the stack height).
- the final component to be modelled is the ambient air at the pipe outlet; it is modelled with the "moist air constant temperature, pressure and humidity source" component, setting again the ambient temperature to 25°C, the ambient pressure to 1.013 bar and the relative humidity to 70%.

For this application an open cathode fuel cell was chosen: it differs from the traditional layout because usually the air compressor is used in the oxygen supply system. It has three disadvantages that can be erased, to maximize the boat performances:

while the other part is useful to keep the electrode wet. As happens in traditional fuel cells, a fraction of the water, produced at cathode, is transported to the anode through the bipolar plate via electro-osmosis, making even the anode electrode wet.

3.5 Hydrogen supply system

The most critical aspect of a fuel cell is the hydrogen supply to the electrode, if it is too low the stack can't handle with the power demand, if it is too much it can cause a waste of fuel.

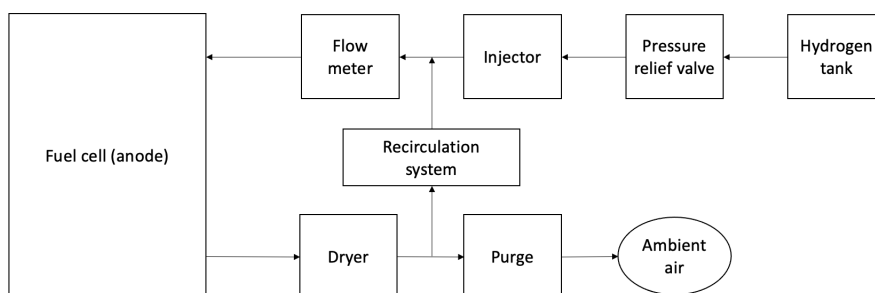


Figure 3.5: Hydrogen supply system scheme

As seen in chapter 1, hydrogen is usually stocked inside high pressure tanks (350 or 700 relative bar). So the first component to be modelled is the tank: it is component of the fuel cell library, that basically is a sum of a gas mixing chamber and a relief valve, both part of the gas mixture library. The rules of the race [7] state that the maximum allowed hydrogen pressure is 700 bar, so that value was used. Then the outlet pressure has to be designed: since at the cathode side the air pressure was just a bit greater than the ambient, the hydrogen pressure must be similar to not generate a significant pressure force difference on the electrodes: so it is set to 1.1 bar. After that it is placed a small chamber, which has to imitate the common rail, as seen in chapter 1 with liquid fuels.

The following component is an injector, modelled using a $2\sqrt{2}$ proportional valve, with maximum opening area of 250 mm^2 ; its position is commanded by the control system, in order to deliver to the fuel cell anode the necessary amount of reactant. As said for oxygen is valid here too, so, to check that this happens correctly, a flowmeter is placed right after the injector and its signal is delivered to the control system.

Hydrogen arrives in the fuel cell chamber, which has a 4L volume, modelled using the mixing chamber of the gas mixture library. Fuel passes through a GDL that endorses hydrogen diffusion towards the electrode. The material is called SIGRACET, made by SGL Carbon GmbH [11]. It has a thickness of 0.8 mm, a

surface of 3660 cm^2 , a permeability of $2.8 \cdot 10^{-12} \text{ m}^2$ and a porosity of 0.82. On the other side of the cathode chamber, the purge system is modelled: it is basically made of a restriction with variable diameter, adjusted by the control system, that, after a certain time, opens, connecting the chamber with the ambient air. The maximum opening area is 28 mm^2 . Purge pipe is very important to let all the hydrogen impurities go away, that can come from the hydrogen tank (residuals from the steam reforming), or can permeate into the anode chamber from the cathode one through the electrode membrane (N_2 or oxygen ions, which forms water); if the first two stayed in close to the electrodes, they would decrease the fuel cell efficiency or could damage the plates. Because of the electroosmosis, both water and nitrogen could migrate to the anode chamber of the fuel cell, occupying some reaction active sites and thus lowering the fuel cell efficiency. Nitrogen, as seen before, could be removed with the purge, while water is removed using a dryer. It is important to say that water is not so dangerous for the electrode itself, but it could drop the performance of the ejector. Since the purge would cause a waste of hydrogen too, a way should be found to limit the fuel quantity that goes out from the fuel cell system. This is the main goal of the recirculation system. Part of the hydrogen, that could exit from the purge pipe, is instead guided into the recirculation pipe, to be delivered again in the anode chamber. Since the downstream pressure of the recirculation pipe is higher than the upstream one, a device is used to force the hydrogen to follow that path. Two tools could be commonly bought: a volumetric compressor or an ejector.

- The volumetric compressor allows to move a certain volume of gas every round, from the upstream part of the circuit to the downstream one, winning the pressure difference. It is driven by an electric motor and its speed could be adjusted to fit every operating condition of the fuel cell, making this component very versatile. Its drawback lies in the cost of all components and in the fact that it consumes energy to work.
- The ejector final result is the same as the compressor, but just using some physical laws and no energy. Basically, the driving jet, that arrives from the injector at high speed, creates a depression at the recirculation pipe outlet, thus generating a positive pressure gradient between the upstream and downstream part of the circuit. Although the ejector is quite cheap, it has a great disadvantage: it works correctly just in a little operating range, because its dimensions are fixed, so it has to be well dimensioned and designed to have the best performance in the desired interval of the fuel cell power outputs.

In the end, the disadvantages of the compressor are judged worse than the ejector ones, especially in a race, where the operating points could be studied before and every waste of energy could be vital.

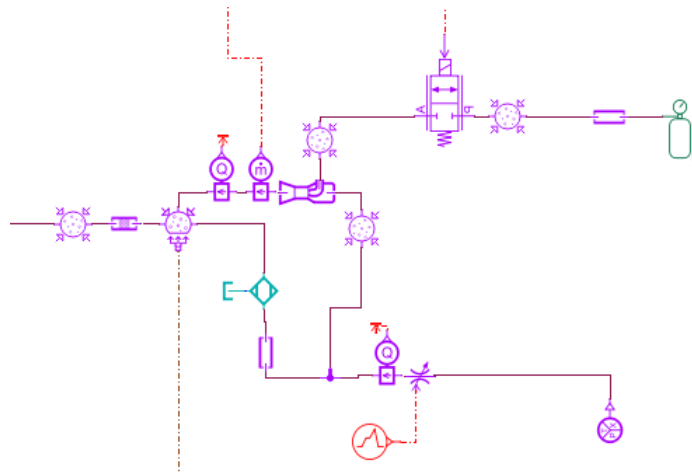


Figure 3.6: Hydrogen supply system model

3.6 Cooling system

The global reaction 1.8 is exothermic, and, as happens in engines, temperature has to be limited. A high temperature is useful for the efficiency (with a benefit in the kinetic of the reaction), but if it overcomes a certain temperature (usually 80°C for PEMFC) there is a reduction of the diffusion efficiency.

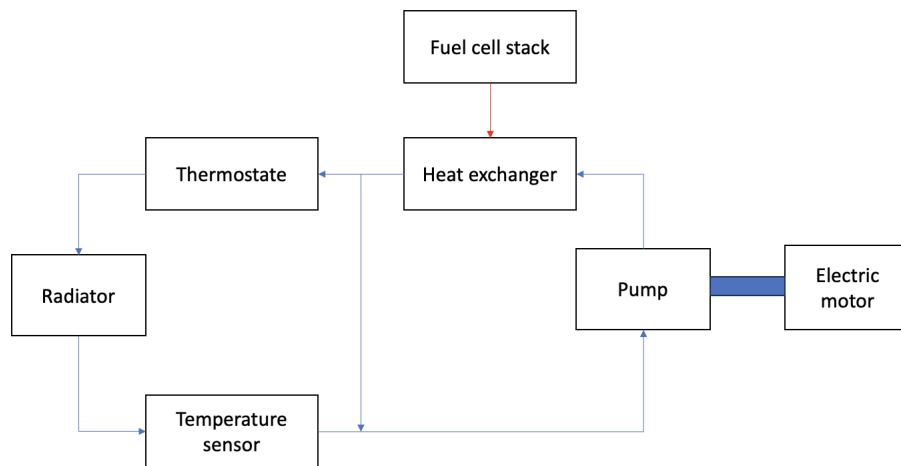


Figure 3.7: Cooling system scheme

The component that simulates the entire fuel cell mass is the stack component, which belongs to the material library. Thus the material proprieties have to be set: Amesim includes a list of materials, whose physical properties are already uploaded;

AISI 316 (the actual stack material) is one of those.

The stack component is connected to the fuel cell component, whose output is the temperature, that becomes a state variable for the stack component. It has three other ports: two convective ports, that simulate the convective heat exchange between the stack and the air and hydrogen chambers, and a coolant ports, that simulates the heat exchanges with the pipes of the coolant system. Its temperature must remain under 67°C , as indicated in the datasheet [10], so the target temperature of 60°C was chosen [10].

All the other components belongs to the thermal library.

- First of all, the coolant has to be modelled: a mixture of water and ethylene glycol, in percentage of 50% each, is indicated in the datasheet. All coolant properties are already saved in Amesim database.
- The pump is the first component to be activated, rigidly connected to a 25 W electric motor, that receives a torque command from the control system: the more the stack temperature is greater than the set value, the greater is the torque command.
- The heat exchanger is modelled as a long circular pipe, whose hydraulic diameter is 15 mm and length is 7 m (because it has to round all the fuel cell stack 8 times) with convection heat exchange port. Pipes are made in steel, with wall thickness of 5 mm.
- The components that controls the coolant flow is the thermostate: it continuously check the coolant outlet temperature from the heat exchanger, and it regulates its opening percentage depending on it: if it is lower that 55°C , it is fully closed and the coolant goes back to the pump inlet, while if it is 60°C or greater is reaches its full opening to the radiator.
- The main component of the whole system is the radiator: it is basically a heat exchanger with the ambient, with a fan that rises the air speed that interacts with the coolant pipe and it's the main component for the air supply system to the fuel cell electrodes. About that, the ambient air speed and temperature are two input signals to the radiator, modelled with the "air velocity and ambient temperature source". The equivalent area of the radiator pipe is 80 mm^2 , its height is 100 mm, its length is 170 mm, the internal diameter of the fan is 90 mm, while the external one is 230 mm. Since its goal here is to maintain the coolant temperature under 59°C , fan just activates when

temperature rises above it and it stops when it drops under 57°C . The power absorption of the fan is 65 W.

- Directly connected to it there is the coolant expansion tank, that is modelled using the accumulator component. It has a total volume of 1L, while the total radiator has a total coolant volume of 2L.
- Just after the radiator, a temperature sensor is mounted: it is vital for monitoring the outlet temperature from the radiator; its signal is directly taken by the control system.

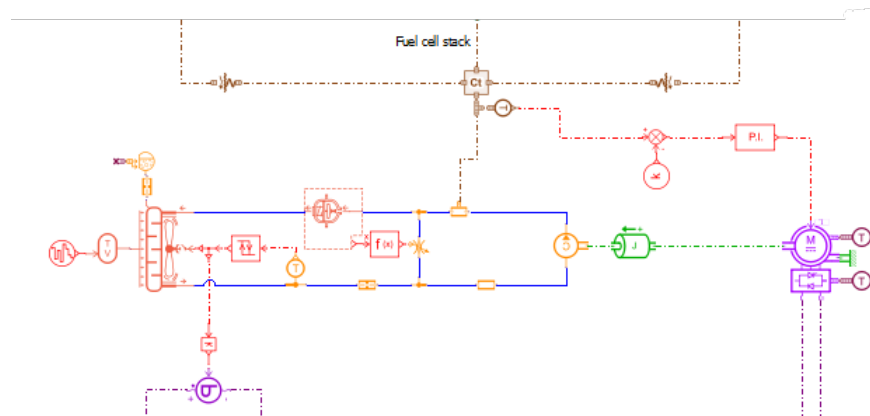


Figure 3.8: Cooling system model

3.7 Electrical system

The fuel cell electrical system is responsible for the correct energy supply to the fuel cell: in particular, the energy that fuel cell produces using an electrochemical strategy can exist just if all the reactant and product of the reaction are controlled.

As can be seen in figure 3.9, a 12V battery handles all the systems, whose components are connected in parallel to it:

- air supply system and cooling system: the electric motor that regulates the fan has a power demand of 65 W
- cooling system: here one electric motor is needed, to move the coolant pump (which is a 25 W motor)
- hydrogen supply system: since the injector in an electrovalve, it has to be connected to the battery to work.

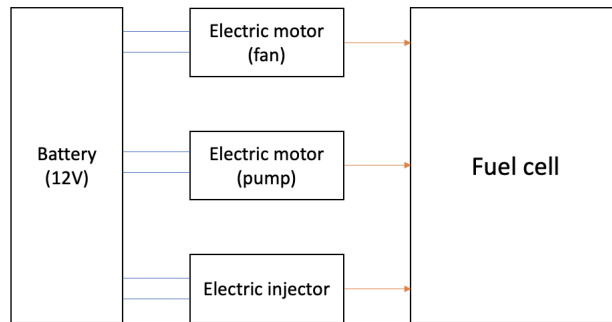


Figure 3.9: Electrical system scheme

In figure 3.10 the electric motor model is shown: the component name is "functional electric drive with separated inverter losses", it belongs to the "Electric motors and drives" library and it has various ports. The two at the bottom are the electric ones (in DC current). Just above, the inverter is schematised, with its own losses; here the component needs the external temperature input. Then the actual motor is included, with four ports: one temperature input, one torque command input, the stator speed input (that is set to zero using a "zero omega" component, from the 1D mechanical library, and the rotor speed output (while the model produces the torque output).

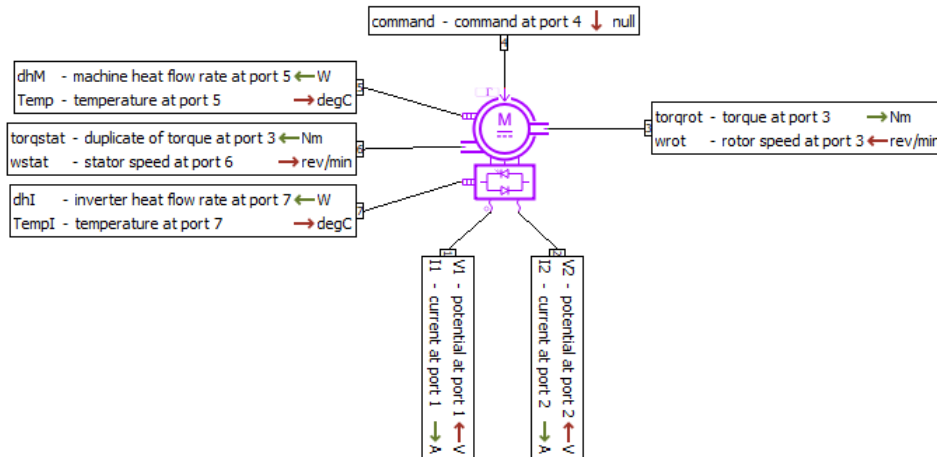


Figure 3.10: Electric motor Amesim component

It is important to notice that the electrical connections make all these components just able to work, but the control system actually adjusts and activates them when it needs.

3.8 Control system

Control system is vital to adjust, in an effective way, the fuel cell in all its operating range. It has to be as more efficient as possible, to avoid waste of fuel and energy. Everything is managed by the ECU (electronic control unit), that uses all inputs, that arrive from the sensors inside the fuel cell, to do very fast calculations, whose final result is an output signal for an electric component, seen in the previous chapter 3.7.

- The air supply system is very important because oxygen has to be always present at the electrodes to allow the reaction to proceed. Since oxygen is directly taken from the ambient air, there is no lack of it, but it is important, to avoid energy waste or, on the other side, oxygen starvation, that the fan is activated at the correct time. In an open cathode, the activation of the fan is usually controlled by cooling demand (especially if the cell is installed in a boat that moves and thus generates a relative velocity with the surrounding air), but sometimes the fan could be activated just to refill the cathode chamber, for example if the speed of the boat is low (or zero) and cooling is not a problem. The control strategy is simple: if the necessary current that the fuel cell has to produce is known, the oxygen amount, that electrodes need to complete the reaction, can be calculated. Thus, a current sensor is mounted at the fuel cell outlet, to know, instant by instant, the current (I) demand.

This signal is transmitted to the ECU as an input. Some very useful Amesim components are the receiver and the transmitter (see figure 3.12, who can, as their names say, pass a signal from one to the other, but without any visible line, simplifying the scheme. After the receiver the "first order lag" component is positioned (see figure 3.12): basically it let the signal pass just every 0.01 s; it is necessary to avoid algebraic loops, mathematical loops where the system can't directly calculate every state variable, but has to create a "fake variable" to complete the simulation; that may slow down the simulation: sometimes it happened that it lasted more than one hour, while, after inserting the first order lag, just five minutes.

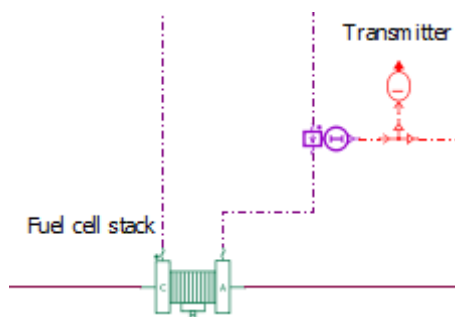


Figure 3.11: Transmitter of current signal model

Once the current signal i arrives to the ECU, some calculations are made.

$$v_{O_2} = \frac{i \cdot N}{4 \cdot F} \quad (3.1)$$

where n is the reaction speed, in terms of oxygen moles consumed per second to produce the current i . N is the mole of electrons that are produced for every mole of molecular oxygen, which is four; it is easy to see in equation 1.5. F is the Faraday constant, already explained in chapter 1.5.

After that, from the reaction speed, the mass of hydrogen consumed per second \dot{m}_{O_2} has to be calculated:

$$\dot{m}_{O_2} = v \cdot M_{O_2} \quad (3.2)$$

where M_{O_2} represents the molar mass of molecular oxygen, and its value is 32 g/mol. Unfortunately this air flow rate would be sufficient just in an ideal system: as a matter of fact, a lot of oxygen that arrives in the fuel cell chamber isn't used and goes directly to the outlet pipe. The ratio between the mass of oxygen that enters inside the chamber and the mass of the one that effectively becomes a reactant is called stoichiometry λ ; its value may be commonly considered 2. Moreover, since the system is an open cathode, with a continuous

air flux, it could be wise to include even an other safety coefficient $CS=2$. To sum up, the estimated oxygen flow rate that has to be delivered to the fuel cell chamber is:

$$\dot{m}_{O_2,tot} = \dot{m}_{O_2} \cdot \lambda \cdot CS \quad (3.3)$$

Since air is made up by the 21% of oxygen, it is possible to calculate the necessary ideal air mass flow rate that produces the demanded electricity:

$$\dot{m}_{air} = \frac{\dot{m}_{O_2,tot}}{0.21} \quad (3.4)$$

The air mass flow rate is measured in g/s. All these calculations are made in the model using two components called "gain". After those, a component called "saturation element" was inserted: basically, the minimum and maximum value of the demanded flow rate can be set; in particular, the minimum one is set, because at the start of the system (since the current of the fuel cell is zero) the requested flow rate would be null.

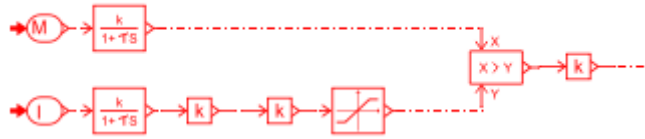


Figure 3.12: Oxygen control system model

The result of these calculations is compared directly with the actual air mass flow rate (M), which is an output from the radiator fan. The "comparison operator" component is used: if the X input (the measured mass flow rate) is higher than the Y input (the estimated necessary flow rate), a signal of magnitude 1 is generated, to send to the fan an activation command. Since it would be a waste of energy making the fan rotate at its nominal speed, this signal is multiplied by 0.3 (using the "gain" component K), to make it rotate just at 30% of the nominal speed.

- The hydrogen system has to deliver the fuel to the anode chamber, trying to reduce waste as much as possible, guaranteeing the highest security level for the pilot. The injection control strategy is very similar to the oxygen control one: since the current demand is known, and since the equation 1.7 remarks that every mole of molecular hydrogen generates 2 electrons (so $N=2$), using the same equations as before it obtained that:

$$v_{H_2} = \frac{i \cdot N}{4 \cdot F} \quad (3.5)$$

$$\dot{m}_{H_2} = v \cdot M_{H_2} \quad (3.6)$$

The molecular mass of H_2 is 2.06 g/mol.

$$\dot{m}_{H_2,tot} = \dot{m}_{H_2} \cdot \lambda \cdot CS \quad (3.7)$$

As before, it has to be noticed that not all fuel that enters inside the electrode chamber will react, going out from the purge pipe instead. Purge is a usual operations for hydrogen fuel propulsion systems, because, as seen in chapter 1, fuel produced by steam reforming can contain some dangerous gases for the fuel cell (as CO) that can't be completely erased by filtering and thus they are present in hydrogen tanks. So it is usual to do every 150-200 s (as suggested in the datasheet [10]) a purge cycle, opening the outlet pipe towards the ambient air. As in the previous chapter, a mass flowmeter is mounted and the measured flow rate is compared to the requested one. The error is analysed by the PI controller and its signal is sent to the switch component: it generates an output that switches from a value (called low value) to another value (called high value) when the input is greater or equal to a certain threshold. Basically, when the PI output is above or equal to 0.1, the switch output is 10 (value chosen because it is actually the current value of the signal that activates the electrovalve, whose rated current is 10 mA), while if the output from PI is lower than 0.1, the switch output is 0, so the injector remains closed.

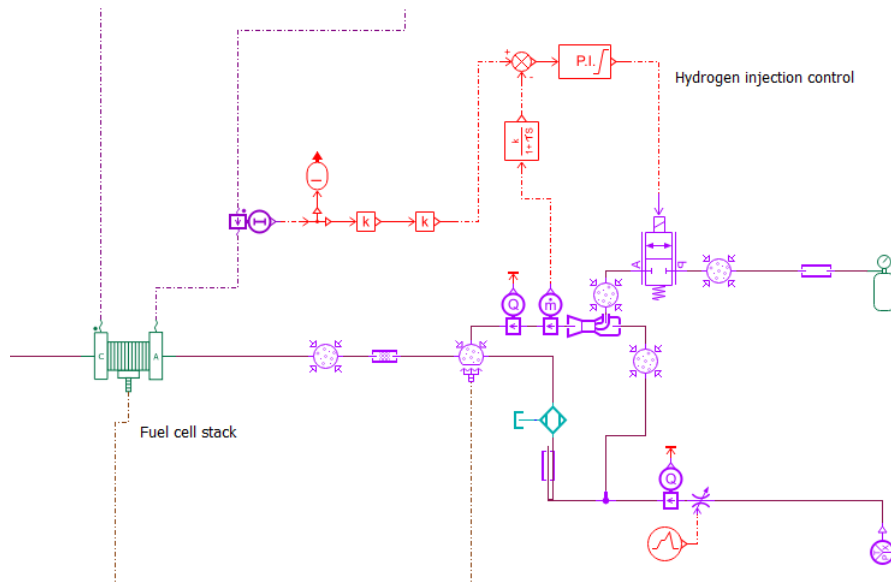


Figure 3.13: Hydrogen control system

- The cooling system is vital to not cause overheat of the fuel cell stack or, more simply, to maximize the cell efficiency controlling the temperature.

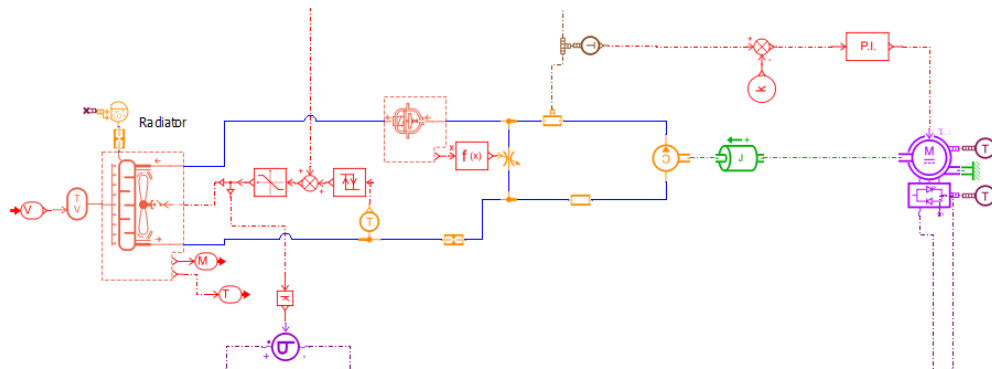


Figure 3.14: Cooling system control model

A sensor measures the fuel cell stack temperature, which is compared to the target temperature, 60°C (since the maximum temperature of the cell is 67°C [10]). The difference between the measured value and the target one is the PI controller input, whose output is the torque command for the electric motor: the goal of the PI controller is to regulate the speed of the motor (rigidly connected to the coolant compressor) and thus the coolant flow rate inside the heat exchanger of the stack, to make the stack temperature equal to the target one.

The component that regulates the coolant flux is the thermostat. As told in chapter 3.6, the percentage of opening toward the radiator depends on wax temperature: if it is lower than 55°C the pipe is fully closed, if it is greater than 60°C , it is fully opened. Furthermore, the opening percentage is transmitted as a signal to the ECU and here it is subtracted from the value 1. The result of the subtraction becomes the input signal to a variable restriction pipe. To sum up, if the thermostat opening percentage is x , the restriction pipe is $1-x$. In this way, if the coolant is too cold (because the stack temperature is lower than the target one), it doesn't enter into the radiator, but it continues to flow in a circle, becoming hotter and hotter until it reaches 55°C , making the thermostat valve opening.

After the radiator outlet, a temperature sensor is mounted and its signal is the input for the trigger component: if the coolant temperature is greater than 59°C , the trigger sends the activation command to the radiator fan, while, if it decreases under 57°C , a deactivation command is delivered. This is a discrete output (0 or 1), and the motor is already integrated inside the radiator component. The signal coming from the air supply control system is summed to this signal, so that the fan activates to prevent air starvation or to lower

the coolant temperature. After the sum, the "saturation element" component is inserted, to limit its input to the maximum value of 1. To simulate the power absorption of the motor of the fan, a power generator component (with a -65 W magnitude) is connected to the 12 V battery.

Chapter 4

Boat propulsion system

After the fuel cell model has been completed, the boat propulsion system has to be modelled; the stack is electrically connected to the propulsive motor, which makes shafts and gears rotate and finally move the propeller. A boat navigation resistance is then connected to the propeller and, thanks to this, the movement of the boat can be analysed.

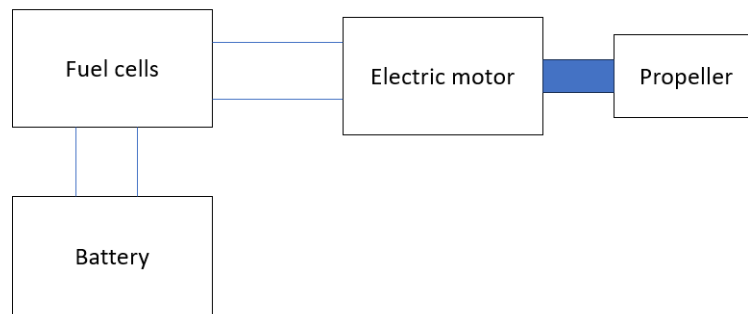


Figure 4.1: Propulsion system scheme

Here another definition component has to be used, the "Sea water properties with sea route option" shown in figure 4.2: it defines the sea water properties, like kinematic viscosity ($1.88 \cdot 10^{-6} \text{ m}^2/\text{s}$) and density ($1026 \text{ kg}/\text{m}^3$); furthermore it defines an index that will be used in the propeller and boat resistance components to identify the ship.



Figure 4.2: Sea water properties definition

4.1 Electric motor

The power produced by the fuel cells is totally directed to the electric motor. The cells are connected in parallel, so the output voltage of each fuel cell is the same, while the total output current is the sum of each output current. After that, a converter is placed, using the "simple DC/DC converter" component, with the output voltage command. This element is very important, since a higher voltage increases the motor efficiency. The converter output voltage (which is the motor input) is set to 400 V. Its efficiency is set to 0.95. Then the actual motor is placed; the "functional electric drive with separated inverter losses" component is used: since the current produced by the fuel cells is a continuous one (DC), there must be an alternator to switch it in an alternating current (AC), so that it can be used by the motor. The Amesim component has five ports:

- two electric ports, for the inlet and outlet DC current, connected to the alternator in the sketch
- one port that simulates the stator rotation, who is connected to the "zero omega" component, to impose on it a non-rotation constraint
- one port that simulates the rotor, that will be connected to the "SHAFT" component, that is the first transmitter of the output motor torque.
- one port that is an input for the signal of the torque request. It is very useful to impose a drive mission.

The motor performances are shown in the table 4.1 below:

Nominal Maximum Power	3.7	kW
Nominal Efficiency	0.9	
Maximum Torque	60	Nm
Maximum Rotor Speed	1250	rpm

Table 4.1: Electric motor performances

4.2 Boat drivetrain

The motor torque and speed are transmitted to the propeller by a sequence of shafts and gears. The boat used in the race is a catamaran, so the electric motor has to be necessarily placed above the water level. Since the axis of the propeller, to maximise the thrust, has to be parallel to the water plane, an L mechanical structure has to be used; it is shown in figure 4.3, while it is modelled in figure 4.4.

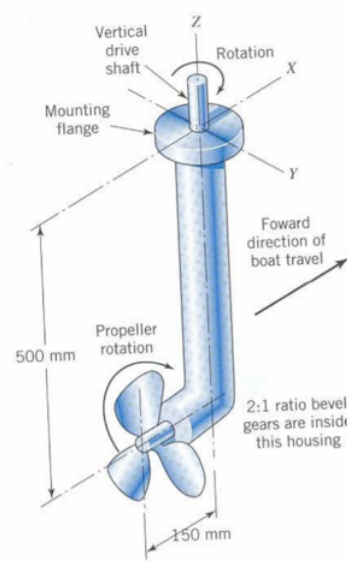


Figure 4.3: Boat drivetrain drawing

The main components are two couples of conical gears, with a respective rotation angle of 90° . Gear ratio was calculated by Amesim in the following way:

$$\tau = \frac{C_{out}}{C_{in}} \quad (4.1)$$

The algebraic sign of the gear ratio in the Amesim model is positive if the inlet torque has the same direction as the outlet one. The first couple, modelled with the "gear ratio (velocity port 1 input)" component, has a fixed gear ratio of 4, while the second one, modelled with the "variable gear ratio (velocity port 1 input)" component has a variable gear ratio, depending on the boat gear: in fact, a boat has three gears, forward, neutral and reverse and the last gear (also called inverter-reducer) must fit the driver's will.

Thus, the reverse gear ratio was set to 1.1, the neutral gear ratio to 0 and the forward gear ratio to -2.1. Even if the inverter is used with just one gear ratio in the endurance trial and in the one-lap race, it is vital to have sufficient manoeuvrability of the boat in the first test that has to be faced, called manoeuvrability test. In the model, the gears are connected by one shaft modelled using the "rotary load with optional friction and endstops" component. It has an inertia of 0.1 kgm^2 and a rotational friction of 0.1 Nm/rpm . The last gear is instead directly connected to the propeller, which rotation speed determines the thrust that makes the boat move.

The last component of the drivetrain to be modelled is the propeller. All the previous gears have the goal of making it rotate faster as possible, delivering the

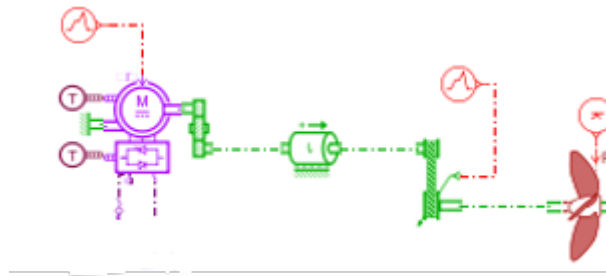


Figure 4.4: Boat drivetrain model

highest possible torque to maximise its rotational acceleration. It is modelled using the "1D marine propeller" Amesim component. A correct propeller design is fundamental, since even a single parameter can make the difference between a slow boat and a fast boat. The first parameter to be set is the pitch: in the model, it is represented by the constant input of the "constant signal" component at the propeller component. All the designed parameters are represented in table 4.2

Propeller Pitch	0.65	m
Rotation Direction	Clockwise	
Propeller Diameter	0.45	m
Blade Area Ratio	0.65	
Number of Blades	3	

Table 4.2: Propeller main parameter

- The propeller pitch represents the distance that the propeller would cover forward in one complete rotation if it were moving through a soft solid material. It has an influence on boat speed: a higher pitch usually brings to a higher speed.
- The rotational direction is a propeller characteristic. It is called clockwise, when, seeing the boat from behind, the propeller rotates clockwise, while it is called anticlockwise, when, seeing the boat from behind, the propeller rotates anticlockwise.
- The propeller diameter is an important parameter for the boat thrust and thus acceleration: a great diameter usually causes a higher thrust than a smaller one. The best propeller is made by a trade-off between a satisfying pitch and diameter dimensions, since, usually, a smaller diameter causes a lower pitch.
- The blade area ratio is a parameter used to relate the size of a propeller blade

to its diameter; it is critical to the control of cavitation and changes in its value cause changes in the propeller efficiency and thrust generation [13].

- The number of blades influences the thrust of the propeller (more blades produce more thrust) and the drag force (more blades cause more drag); thus the best trade-off was found in 3 blades propellers.

All these parameters are used by the Amesim model to calculate thrust and torque. the "four quadrants-Woodward method" was chosen to compute them. They use the ratio between pitch and diameter and the parameter β and a 2D table. The value of the parameter is the following:

$$\beta = \arctan\left(\frac{V}{0.7 \cdot \pi \cdot n \cdot D}\right) \quad (4.2)$$

Where V is the propeller speed of advance, n is the number of blades and D is the propeller diameter. β represents the angle of a line in a four quadrants diagram, with the rotation speed as X axis and the speed of advance as Y axis

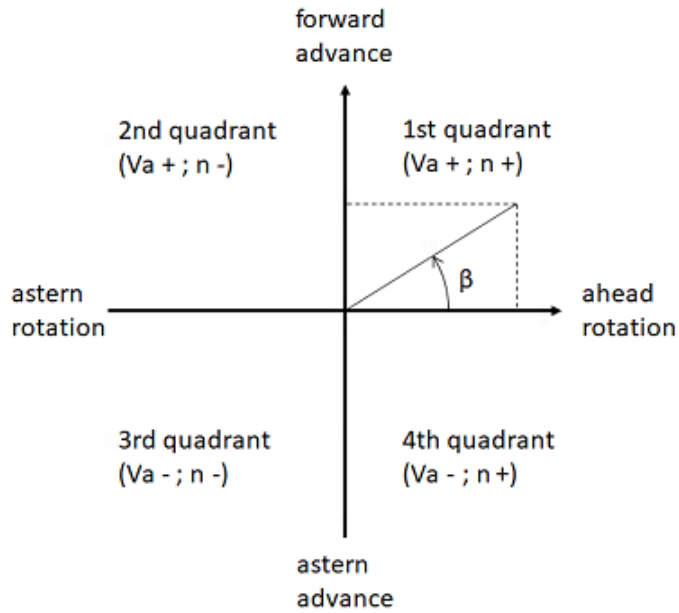


Figure 4.5: Four quadrants diagram [9]

Usually the second and third quadrants are not used; if the line is in the first quadrant ($0 < \beta < 90^\circ$) the advance speed is forward if the rotational speed is ahead, while if the line is in the fourth quadrant ($270^\circ < \beta < 360^\circ$) the advance speed is astern if the rotational speed is ahead.

4.3 Boat resistance model

After all the powertrain system was modelled, it has to be mounted on the boat. In Amesim that could be made very easily, just connecting the "1D marine propeller" with the "ship model with navigation resistance" component. This last element has another force input port, that could be used if the boat is towed; in this model the catamaran moves on its own, so that port is connected to a "zero force" component. Thus, the complete powertrain model used for the simulation is shown in figure 4.6.

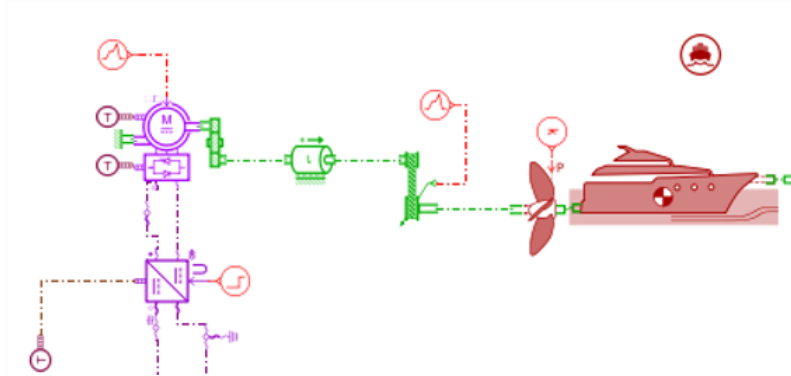


Figure 4.6: Powertrain model

The component is identified with the same ship number, as the propeller, set in the "Sea water properties with sea route option" element. The boat given by the Yacht club de Monaco is a catamaran, one of the less studied types of boats; as a matter of fact, Amesim has not a resistance model of a catamaran and then all the dimensions of the boat should be approximated to try to create a satisfying model. The resistance model needs a lot of data to work; the first one is the boat category, that implies the hull shape too; yacht was chosen, since is the most similar to a regular little boat (and easier to model). Then the total weight is asked: since the hull is 60 kg and only a pilot should drive the boat, 200 kg is supposed. Moreover, the boat dimensions are inserted: they are reported in table 4.3

Waterline Length	5	m
Breadth or Beam	1.2	m
Afterward Draft	0.5	m
Forward Draft	0.3	m
Immersed Transom Area	0.36	m ²

Table 4.3: Main dimensions of the Amesim boat model

All the main dimensions are taken from the Monaco race rules [7] and the

immersed transom area is calculated by multiplying the forward draft and the beam. Usually the yacht hulls have a bulbous bow in the front and some bow thrusters, but in this case all the dimensions of these parameters are set to zero. This component has a current parameter too, but, for this simulation, it is neglected. With all the requested parameters, the total boat resistance is calculated (using the Holtrop and Mennen model, since it is the one that fit better with the boat). The final result can be expressed by the following diagram:

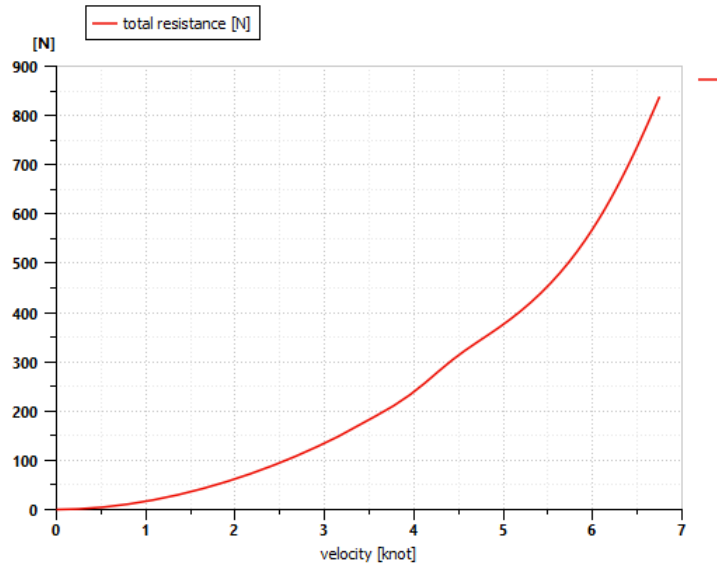


Figure 4.7: Boat resistance of the Amesim model

As imagined the diagram has an exponential trend, similar to the air drag one. Nevertheless the whole model is an approximation; that's why another calculation strategy has been used to check if the Amesim model overestimates or underestimates the resistance value. This is made through a formula, called ITTC-57. It is an experimental strategy, that sums the water drag (calculated by the formula) and the resistance made by the waves that the boat itself generates. At the peak velocity that is studied in this work, the two resistance terms could be considered to have the same value. The technique that is used here is the following: first of all, since a catamaran has two hulls that touch water, just one hull resistance has to be calculated. This result will be multiplied by 2, to consider both the drag term and the wave term. After that, this value will be multiplied by 2 again, to consider both boat hulls. The total weight P of the boat is equal to the Archimedean force, that states that "a body immersed in a fluid is subjected to an upwards force equal to the weight of the displaced fluid". Thus, dividing the water

mass for the water density, the immersed volume of the boat V_{water} is calculated:

$$V_{water} = \frac{m}{\rho} \quad (4.3)$$

This is the total water volume, it has to be divided by 2 to have the immersed volume of just half of the hull.

$$V_{hull} = \frac{V_{water}}{2} \quad (4.4)$$

Then the hull Reynolds number is calculated

$$Re = \frac{v \cdot L}{\nu} \quad (4.5)$$

v is the boat velocity, L is the hull length, while ν is the kinematic viscosity of water ($1.88 \cdot 10^{-6} \text{ m}^2/\text{s}$). Now the actual ITTC-57 formula is used, to calculate the drag coefficient C_f :

$$C_f = \frac{0.075}{\log(Re) - 2^2} \quad (4.6)$$

The total resistance coefficient C_t , as said before, is calculated multiplying C_f by 2:

$$C_t = C_f \cdot 2 \quad (4.7)$$

The drag resistance depends on the wetted surface S of the hull. Unfortunately, without a CAD model or some experimental data, just an approximation of it could be made. Thus, an experimental formula is used [14]:

$$S = C_s \cdot \sqrt{V_{hull} \cdot L} \quad (4.8)$$

The coefficient C_s (the wetted surface contour coefficient) is found using the following experimental diagram 4.8

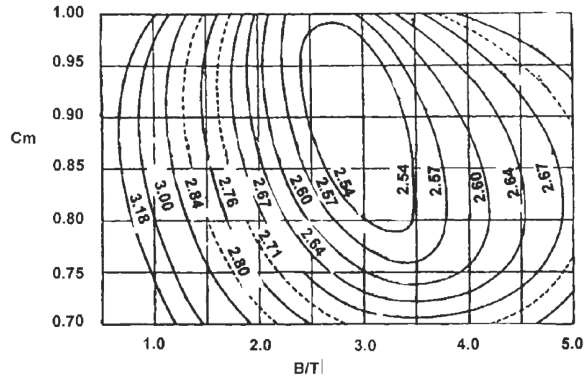


Figure 4.8: Wetted surface coefficient[14]

Since the B/T (Beam to Draught ratio) coefficient is close to 1 and C_m (midship area coefficient) can be considered 0.75, to make C_s have the maximum value 3.18 to be conservative. Thus the drag resistance R_{hull} can be calculated:

$$R_{hull} = \frac{1}{2} \cdot C_t \cdot \rho \cdot S \cdot v^2 \quad (4.9)$$

Boat total resistance R_{tot} is calculated doubling the value of the one for just a hull R_{hull} :

$$R_{tot} = R_{hull} \cdot 2 \quad (4.10)$$

The total resistance of the boat is represented in diagram 4.9 too:

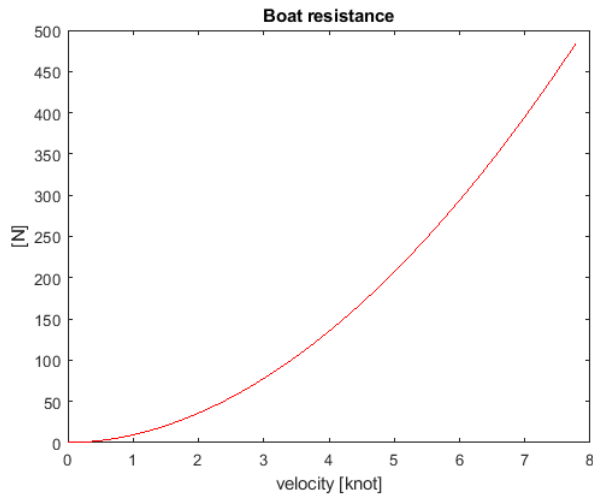


Figure 4.9: Calculated boat resistance

It is easy to see that this resistance, calculated with empirical formulas, has a much lower value than the one estimated by the Amesim model. For this reason R_{tot} has to be considered closer to the real situation; thus the speed of the boat (computed by the model) is probably a bit underestimated.

Chapter 5

Model design through the three trials

5.1 The maneuverability test

As explained in chapter 2, the Monaco energy boat challenge is made up by three different trials: the maneuverability test, the endurance race and the one lap race. The first one is essential to be passed to can join the next two. Here the boat has to overcome a little path in Monaco harbour:

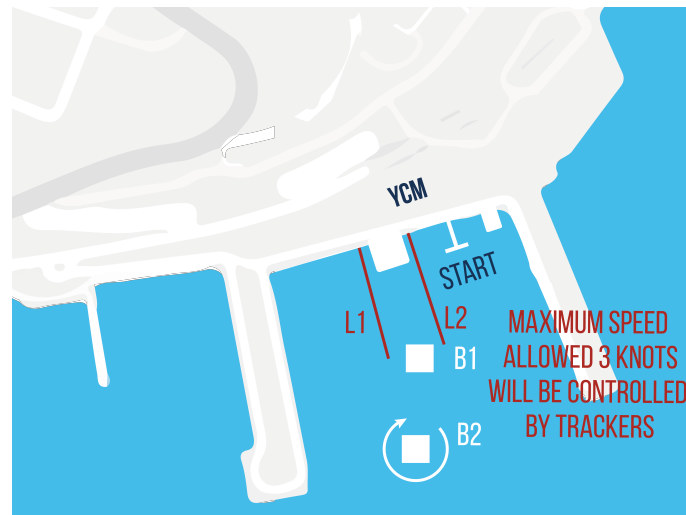


Figure 5.1: Slalom trial course[8]

Driving a boat is totally different from driving a car, because the car driver can control, turning the steering wheel, the vehicle direction in a perfect way in

almost every condition. Instead the boat movement is influenced a lot by waves, currents, and wind. That's why a commercial boat must be advanced enough to be driven by the pilot in the desired direction. Thus, the rudder has to be mounted to make the boat curve, but it can't be modelled in Amesim. Instead a reverse gear can be very useful, both to stop the boat and to turn the bow faster; that is possible because the final gear is an inverter-reducer (as explained in chapter 4.2. For example, a 10 seconds cycle is simulated, in which the electric motor is supplied by the fuel cells to have 2.9 kW of power. At the beginning, for 4 seconds, the reverse gear is used, then the neutral is put for one second; for the rest of the simulation the forward gear is used.

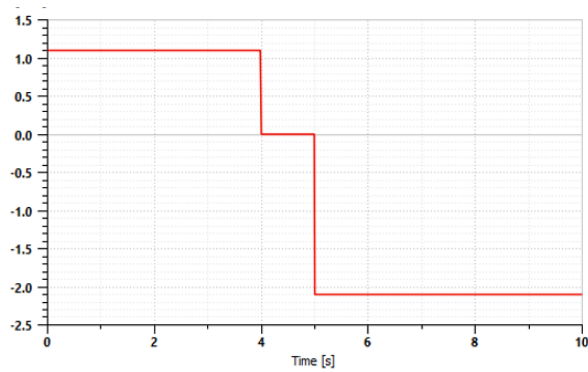


Figure 5.2: Inverter-reducer gear ratio

So, when the pilot selects the reverse gear, the reducer gear ratio changes (in magnitude and sign), allowing the boat to have an astern advance. Instead, when the neutral gear is put, the gear ratio of the reducer becomes zero. The values of gear ratio are described in 4.2. The velocity of the boat is represented in figure 5.3:

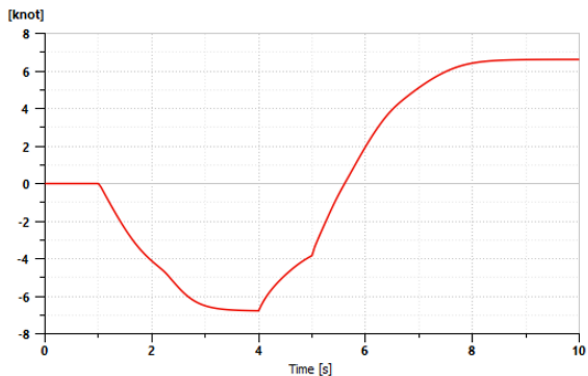


Figure 5.3: Boat speed in a maneuverability simulation

5.2 The endurance test

The endurance test consists of a 4 hours trial, while the runners should complete as many laps as they can. The race path is placed just in front of Monaco harbour and it is shown in figure 5.4



Figure 5.4: Endurance race path[8]

Moreover the points won in this trial are double than the one that can be obtained (with the same ranking) in the 1 lap race. Thus, this race was the real target of the whole design work, trying to optimize the fuel cell boat to reach at least the top 3. As a matter of fact, in 2022, the endurance race laps were 1 nautical mile long and the best participant made 27 laps, while the third 25 [8]. Knowing that the maximum time for the race was 4 hours, the average velocity v_{\min} should have been at least:

$$v_{\min} = \frac{\text{total nautical miles}}{\text{time}} = \frac{25 \cdot 1}{4} = 6.25 \text{ knots} \quad (5.1)$$

The most difficult restriction of this trial lies in the limited amount of energy E_{tot} that can be stocked on board, who is just 10 kWh. In the technical rules of the competition, the following formula is also written [7]:

$$E_{\text{tot}} = \sum f_i \cdot E_i \quad (5.2)$$

In chapter 2 was already told that the energy factor f_i for hydrogen has the value of 0.4. Thus, if only hydrogen was used, the total energy stocked on board as gaseous source would be:

$$E_i = \frac{E_i}{f_i} = \frac{10}{0.4} = 25 \text{ kWh} = 90 \text{ MJ} \quad (5.3)$$

From this value, the total mass m_{H_2} and volume V_{H_2} of hydrogen inside the tank could be calculated:

$$m_{H_2} = \frac{E_i}{H_i} = \frac{90}{130} = 0.692 \text{ kg} = 692 \text{ g} \quad (5.4)$$

H_i is the hydrogen lower heat value, that represents the reaction energy of a kg of hydrogen (not considering the latent heat); it has a magnitude of 130 MJ/kg. Knowing the hydrogen mass, the ideal gas formula can be used to calculate the respective volume, knowing that the hydrogen is pressurised in the tank at 700 relative bar (as the rules allow [7]) and the tank temperature is the Monaco ambient one, so around 25°C

$$p \cdot V_{H_2} = n_{H_2} \cdot R \cdot T = \left(\frac{m_{H_2}}{M_{H_2}} \right) \cdot R \cdot T \quad (5.5)$$

$$V_{H_2} = \frac{\left(\frac{m_{H_2}}{M_{H_2}} \right) \cdot R \cdot T}{p} = \frac{\left(\frac{692}{2.06} \right) \cdot 8.314 \cdot 298.15}{701.013} = 0.012 \text{ m}^3 = 12 \text{ L} \quad (5.6)$$

Unfortunately, even with the recirculation system, not all the hydrogen will react, since part of it will be depleted by the purges. In control system 3.8, the stoichiometry λ is set to 2 to command a higher demand to the injector to avoid starvation, but in these calculations about the reactant usage, it can be considered 1.1 with a good approximation. Moreover the fuel cell efficiency could be considered 0.6: in the Amesim model it is 0.7, but this value is too optimistic for a real stack, for which 0.6 is a more realistic efficiency. So the electrical energy that can be produced by the fuel cell stack is:

$$E_{FC} = \eta \cdot \frac{1}{\lambda} \cdot E_i = 0.6 \cdot \frac{1}{1.1} \cdot 25 = 13.6 \text{ kWh} \quad (5.7)$$

The main power consumption in the boat is caused by the electric motors (both the propulsion one and the auxiliary ones). The auxiliary systems of every fuel cell request the power P_{aux} :

$$P_{aux} = (P_{fan} + P_{pump}) \cdot 110\% = (65 + 25) \cdot 110\% = 99 \text{ W} \approx 100 \text{ W} \quad (5.8)$$

The auxiliary power is raised by its 10% because of the electrical losses. Thus, considering that in the boat there are 3 fuel cells that, in the endurance race, have to work for 4 hours straight, the auxiliary motors energy demand is:

$$E_{aux_{tot}} = P_{aux} \cdot 3 \cdot 4 = 100 \cdot 3 \cdot 4 = 1.2 \text{ kWh} \quad (5.9)$$

Since would be better to use all the energy stocked inside the tank to make the boat move, there should be a way to supply the energy for the stack subsystem:

looking at 2022 boats, solar panels can be seen. This is a really good idea, since the rules just talk about the energy that the boat can stock at the starting line and the energy produced by the panels would be some free bonus energy. Looking into the net, the Ecoflow solar panel (82 x 183 x 2.5 cm) was found; it is said that it can produce a power of 150-200 W.

$$E_{solar} = P_{solar} \cdot 4 \quad (5.10)$$

So for the entire race a single panel can produce 0.6-0.8 kWh. If two of them were used, at least 1.2 kWh would be produced, enough to supply energy to the electric motors (furthermore the panels power would be enough to satisfy the demand of the auxiliaries). In the Amesim model they are simply modelled using two power sources (with the "power source or sink" component, using as input the "pseudo-random binary sequence" component) between 150 and 200, connected to the auxiliary circuit:

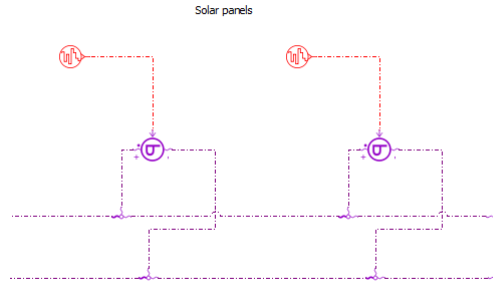


Figure 5.5: Solar panels model

Now the electric motor has to be designed; its target power, for the endurance race, is limited by the total energy stocked inside the boat, calculated in 5.7; Proceeding in an iterative way, the value of 2.9 kW is found to be good: as a matter of fact, the motor power has to be divided by the motor and converter efficiency to found the power demand at the stack:

$$P_{demanded} = \frac{P_{motor}}{\eta_{motor} \cdot \eta_{converter}} = \frac{2.9}{0.9 \cdot 0.95} = 3.39 \text{ kW} \quad (5.11)$$

And multiplied for the 4 hours of the race, the demanded energy is found:

$$E_{demanded} = P_{demanded} \cdot 4 = 13.57 \text{ kWh} \quad (5.12)$$

Thus is checked that

$$E_{demanded} \leq E_{FC} \quad (5.13)$$

So the energy balance inside the boat is satisfied. Now that all the components are designed, the model can run. A simulation cycle of 300 seconds is made and, in the rest of this chapter, some results are shown as diagrams.

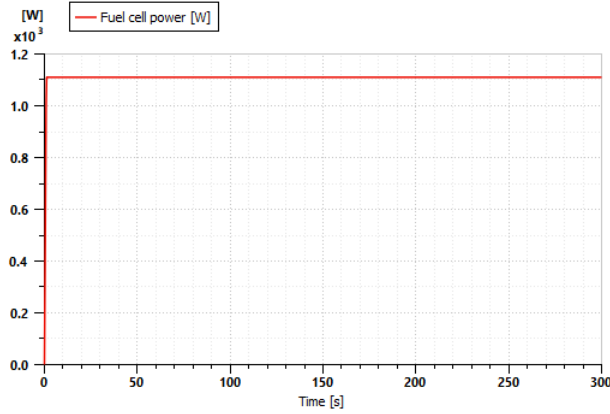


Figure 5.6: Endurance race simulation, fuel cell power

The first diagram (5.6) shows the demanded power to a single fuel cell in the endurance race: the mission is a constant power at the motor of 2.9 kW. To supply that, according to the model, every fuel cell has to produce around 1.1 kW.

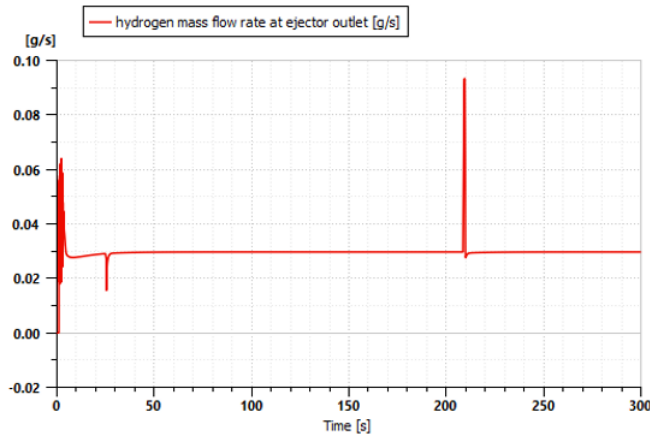


Figure 5.7: Endurance race simulation, hydrogen flow rate

In figure 5.7, the hydrogen flow rate to the anode chamber can be seen. The trend shown in the first seconds is related to the control system, that, every time the injector opens, it almost immediately closes the valve because the flow rate exceeds the requested one, but then a lower flow rate is measured and thus the injector is fully opened again and so on. After 10 seconds the anode chamber pressure becomes already very close to the supplied hydrogen one (1.1 bar) and,

from that moment, the flow rate becomes much more smooth. The huge peak at 210 s is the purge event: the anode chamber is connected to the ambient through a restriction and the chamber pressure becomes lower for an instant, causing a rise in the flow rate.

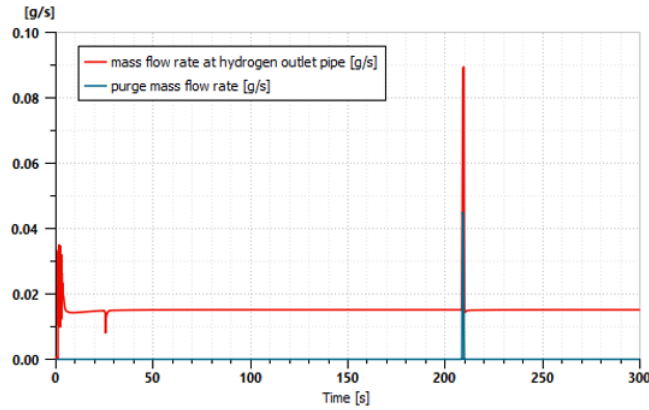


Figure 5.8: Endurance race simulation, recirculation and purge

In figure 5.8 are shown the outlet flow rate from the anode chamber (red line) and the purge flow rate (blue line). As said before, in the first seconds the anode chamber pressure is rising and the inlet hydrogen varies a lot instant by instant. The difference between the outlet hydrogen from the chamber and the one that goes out from the system, because of the purge, is the recirculated hydrogen. It is more or less constant during the simulation, because in those moments the anode chamber is constant and the same is the injector hydrogen flow rate (thus the depression caused by it is the same).

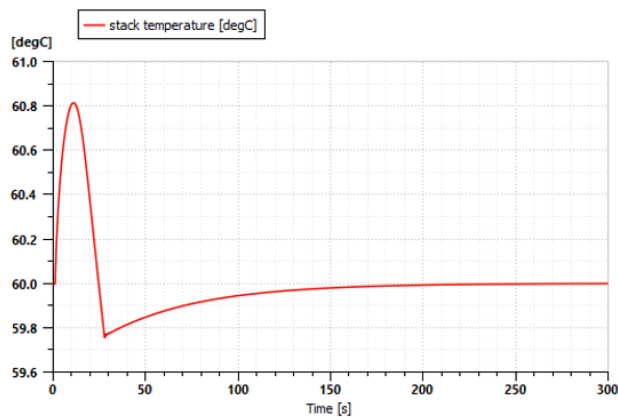


Figure 5.9: Endurance race simulation, stack temperature

In figure 5.9 it is possible to see the stack temperature; the cycle begins with the fuel cell already hot (60°C) and, when it starts to work, its temperature rises. Since the coolant temperature was set to 59°C , even the fan is activated at the beginning and, after a few seconds the temperature of the stack begins to drop; around 25 seconds of simulations, the drop ends and the temperature rises very smoothly again, this time reaching the set point of 60°C .

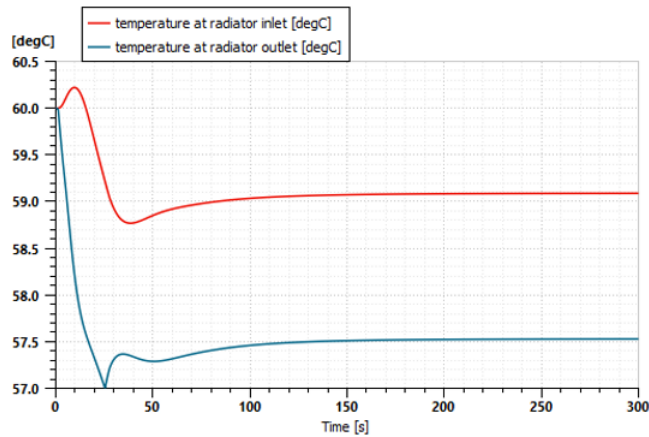


Figure 5.10: Endurance race simulation, temperature of coolant at the inlet and outlet from the radiator

The reason why the stack temperature stops to drop is shown in figure 5.10: while the fan works, the outlet temperature of the coolant from the radiator continuously drops, until it reaches 57°C ; that is the temperature at which the control system stops the fan. As a matter of fact, it can be seen in figure 5.11 that the fan signal becomes zero (and it means that the fan stops to rotate) in the instant when the coolant temperature becomes 57°C .

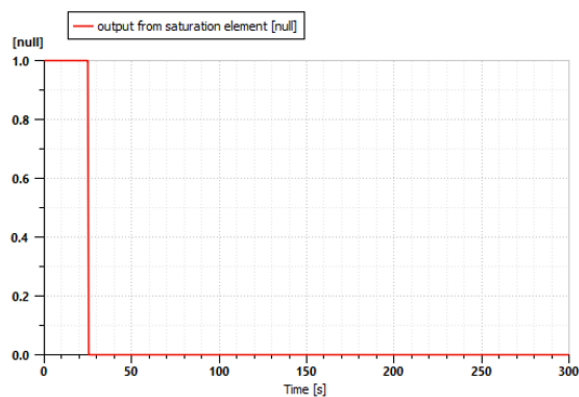


Figure 5.11: Endurance race simulation, fan activation phases

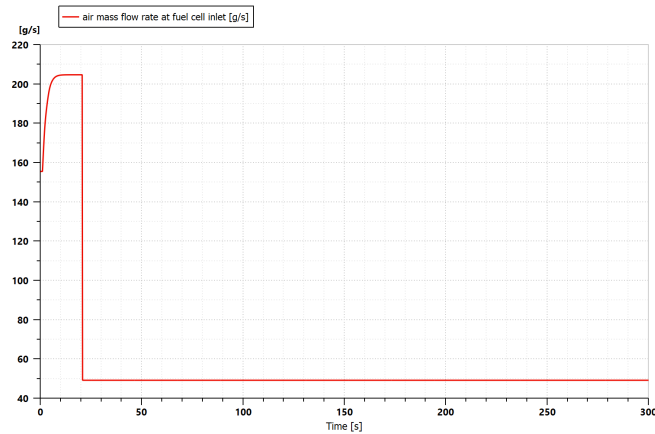


Figure 5.12: Endurance race simulation, air flow rate

In figure 5.12, the air flow rate after the fan is shown; that mass of air cools the radiator pipe and then it enters inside the cathode chamber, at a temperature around 44°C. It can be seen that the air flow rate is much more than the demanded one, but it is because in an open cathode the same air has to be used by the radiator (whose ambient air demand is high) and by the electrodes. Anyway, these are very important results, because it means that the air speed caused by the movement of the boat is enough to cool the stack and to supply air to the cathode electrodes, so a high power demand could be avoided during the race. The last result to be checked here is the boat velocity: it has an effect on the cooling system (as seen before) and, in a race, is the most important number. The model computes a constant speed of 6.54 knots, after a fast transitory, that could be sufficient to reach the goal of joining the top 3.

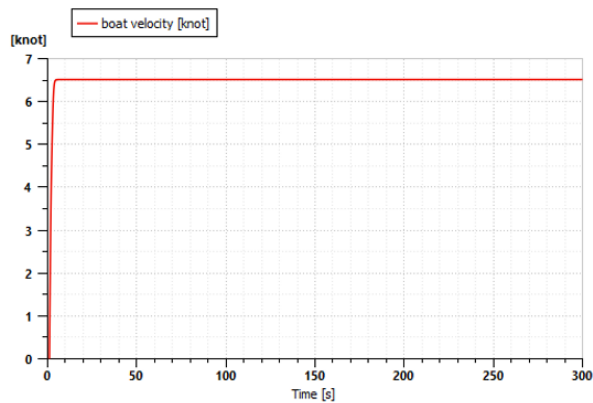


Figure 5.13: Endurance race simulation, boat speed

5.3 One lap race

In the 1 lap race, a 1 nautical mile has to be done, following the same course of the endurance race (in the 2022 edition). This time, the 3 fuel cells have to operate at their highest performance, 1.5 kW each. It means that the power that is delivered to the motor is:

$$P_{motor} = (P_{fuel\ cells}) \cdot \eta_{motor} \cdot \eta_{converter} = (1.5 \cdot 3) \cdot 0.9 \cdot 0.95 = 3.7\ kW \quad (5.14)$$

As done in previous chapter, diagrams, of 300 s in race condition, of the main components are shown. A very few differences appear, basically because the power output of the fuel cells in this race (that can be seen in figure 5.14 is greater but not so different from the endurance one.

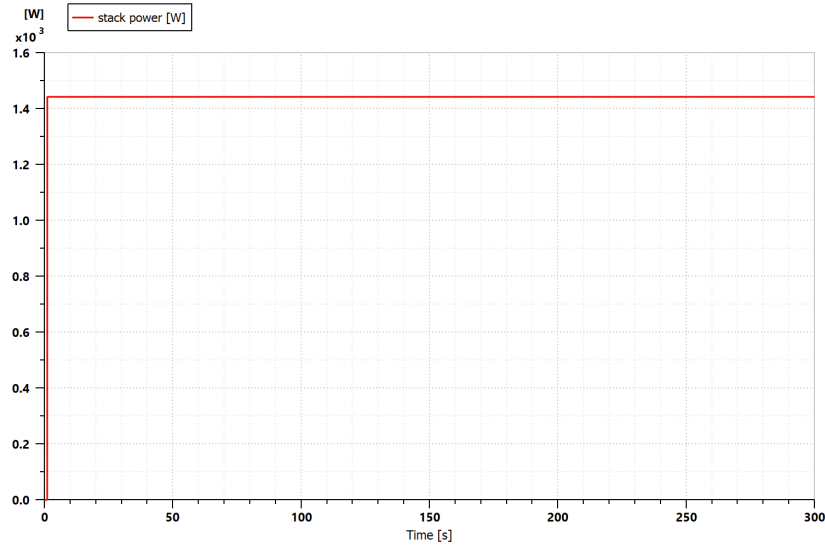


Figure 5.14: Championship race, fuel cell power

The hydrogen flow rate that enters inside the anode chamber is shown in figure 5.15. Since the power demand of the fuel cell is greater, even the requested hydrogen is greater than in the endurance race. As before, after a transitory, the flow rate becomes quite stationary. At 210 seconds of the simulation there is a rise, caused by the activation of the purge system.

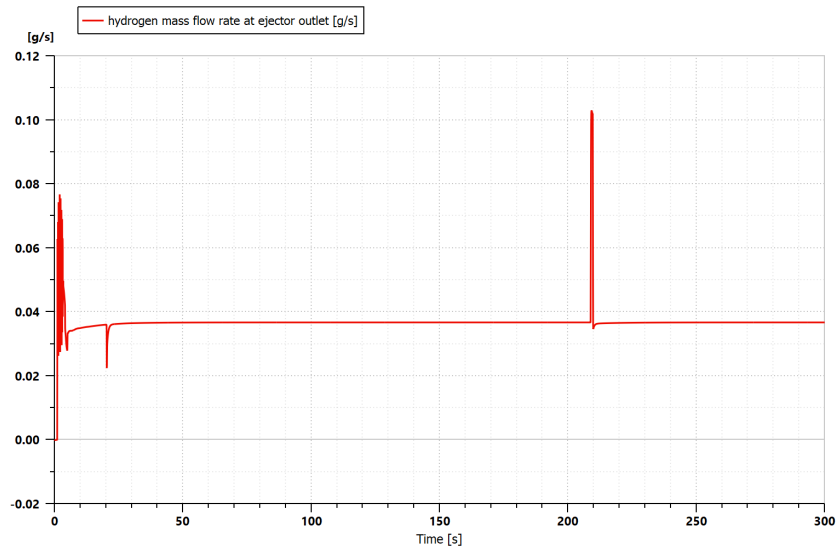


Figure 5.15: Championship race, hydrogen flow rate at fuel cell inlet

Even in this case, the cooling system handles the rise in temperature of the stack during the cell work. Diagram 5.16 shows that it heats up until 61°C, before starting to cool down. Temperature drops until 35 s, where there is an asymptotic rise to the target of 60°C.

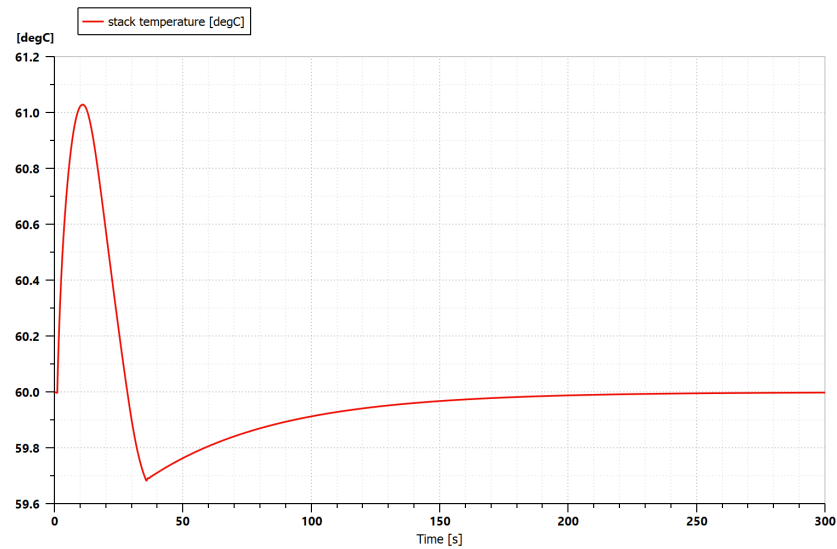


Figure 5.16: Championship race, stack temperature

If the radiator is looked a bit deeper, it can be seen that the radiator works properly for the whole simulation time. At 25 s, the outlet coolant from the radiator

reaches 57°C; it causes the fan to turn off: that is why its temperature rises a bit just after that moment.

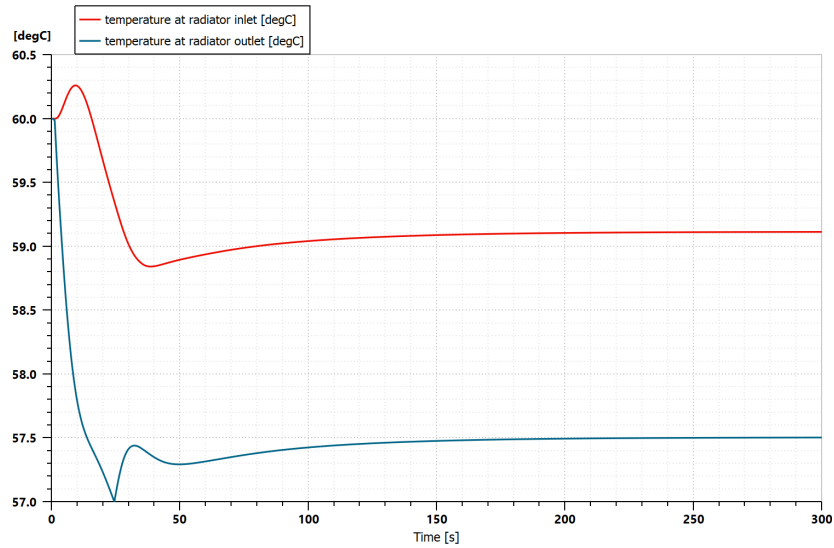


Figure 5.17: Championship race, temperature of coolant at the inlet and outlet from the radiator

Thus, in figure 5.18, the air increase caused by the fan can be seen: as said before, at 25 s, the fan stops because the coolant temperature becomes sufficiently low. It can be noticed that, even in the championship race simulation, the fan, doesn't need to be turned on again; so the movement of the boat is necessary to cool down the coolant and to avoid starvation in the cathode chamber.

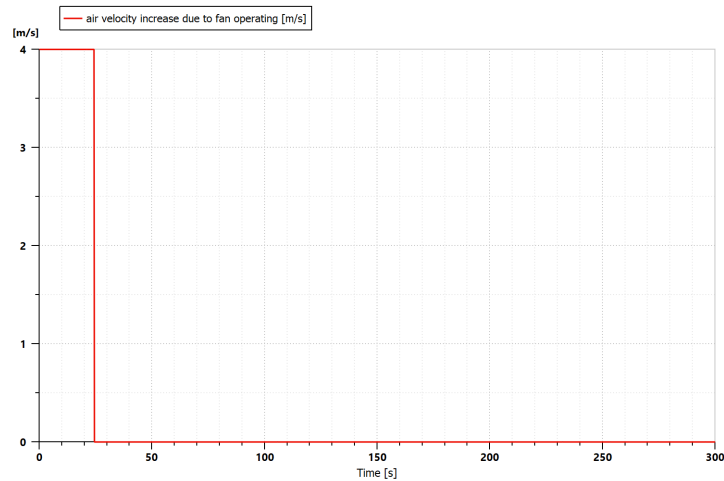


Figure 5.18: Championship race, air speed increase because of the fan

Since the fan stops at 25 s, even the air mass flow rate that enters inside the cathode chamber drops (as can be seen in figure 5.19. It can be noticed that, even in the championship race simulation, the fan, doesn't need to be turned on again; so the movement of the boat is necessary to cool down the coolant and to avoid starvation in the cathode chamber.

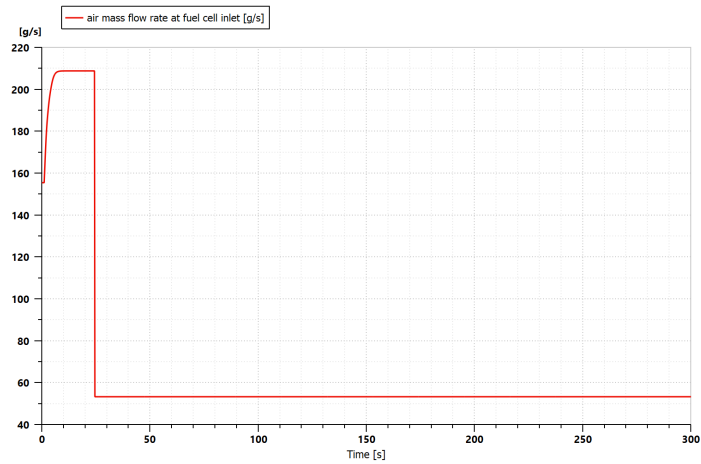


Figure 5.19: Championship race, air flow rate

In this simulation the boat velocity arrives to 6.74 knots, even if (as said in chapter 4.3) the real speed would probably be higher than that.

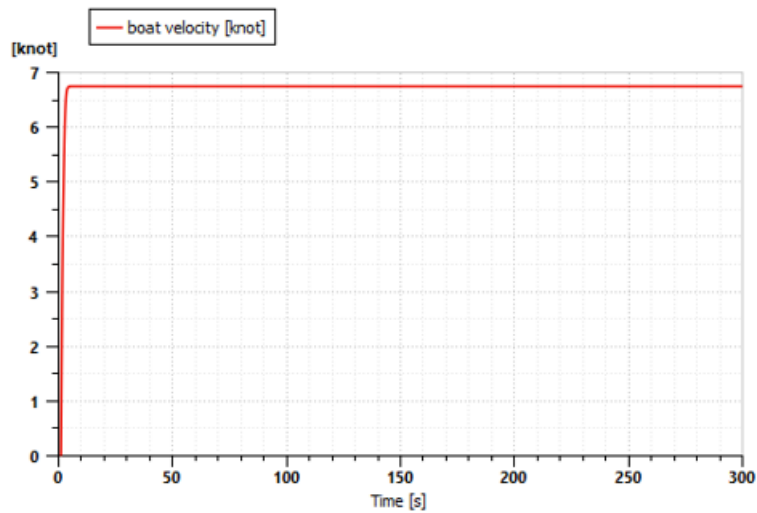


Figure 5.20: Championship race, boat speed

Chapter 6

Conclusions

6.1 Results

An Amesim model of a fuel cell boat was designed from scratch. Every major powertrain component was included in the model in order to assess a specific design requirement set by the competition's rules. More specifically, the fuel cell stack component had to be the energy producer and a real fuel cell [10] was used to have at least a power curve and a range of ratings that could fit the boat; from them, 1.5 kW was chosen and all parameters of the Amesim component were set according to its manual. Fuel cell electrodes need a different supply system for each reactant, so the hydrogen and oxygen supply systems were modelled, both with a GDL membrane modelled. The hydrogen one was made taking, as an example, a conventional one with the tank, the injector, the recirculation system and the purge pipe. Since the fuel cells used are of the open cathode type, to avoid creating a critical pressure difference between the electrode cathode and anode side, the outlet hydrogen pressure from the tank was set to 1.1 bar. To make the recirculation system work, a volumetric compressor or an ejector could be chosen, but the second was preferred because, if it is correctly designed, it has a satisfying performance in the desired operating range, without any electrical power absorption. The purge interval was set according to the manual [10]. Since the fuel cells are open cathode, the air supply system is strictly related to the coolant one, since there is just one fan (see the datasheet [10]) of 65 W that delivers ambient air to the radiator first (since the temperature is still low) and afterwards to the cathode. Since the fuel cell stack produces heat when it works, a coolant system was built: it was modelled following another Amesim model of a car, with a pump (driven by a 25 W motor) to move the coolant inside the pipes, a heat exchanger to cool the stack, a thermostat to regulate the coolant flow inside the whole system and the radiator. The radiator fan is the same as the air supply system, while the

radiator size was reduced from the original one of the car. To make everything work correctly, the control system was modelled: it regulates every main effect of every subsystem, such as the fan activation or deactivation when the coolant becomes too hot or too cold (or, in a few cases, to avoid the oxygen starvation at cathode chamber), the pump speed to adjust the stack temperature to the set value, the hydrogen injected flow rate, to avoid the anode starvation. The reactant flow rate, which should be sent to the electrodes, was calculated from the current produced by the fuel cell through the Faraday constant and the molar masses. So, the fuel cells were modelled and the next step was to connect them to the electric motor and the drivetrain. The drivetrain was made up of two gears and a shaft, and it ends with the propeller; the propeller was connected to the boat resistance model, whose parameters were just supposed and after it was verified (using the ITTC-57 formula and hypothesizing that the drag resistance had the same value as the waves resistance) that the Amesim model overestimated it. The tactic used to set the parameter of the drivetrain components was an optimization one: the model was run, changing a parameter at time, until the best ones were found. The same was done with the motor's maximum torque and speed.

After the model was ready, the energy balance was made; since it is the most important one, the endurance race was chosen as target. Two solar panels were used to produce as much energy as the auxiliary systems need and, as the rules of the race implicitly suggested, a full hydrogen propulsion was used. All calculations can be found in chapter 5.2, but at the end the most powerful motor, that could be used, was a 2.9 kW. In chapter 5.1 was explained why an inverter-reducer was mounted, while in chapter 5.3 the maximum performance of the 1.5 kW fuel cells powertrain was shown.

6.2 Future developments

Since the boat's fuel cells were designed to perform well in the endurance race, the one-lap race ranking won't probably be competitive, as explained in chapter 5.3. The first upgrade to do, it is to check the maximum motor power to reach the top 3 ranking even in the one-lap race, then it has to be checked if it can be supplied by the fuel cells, calculating if the total energy stocked inside the tank as hydrogen is enough to complete the race.

This thesis project has the scope of building a solid base for a future development team in Chalmers, to develop a competitive vessel for the Monaco race in the next years. The model in its present state provides guidance on the performance requirements and dimensions of the majority of the components; thus, when they are bought, a meticulous experimental analysis will be made and all data will be added to the model, to have a more realistic simulation that could even predict,

with a satisfying accuracy, every component behaviour during a race. Furthermore, a lot of troubles will surely happen during the races. From those, a list of problems has to be made, to try to correct them during the winter season. Every year the boat will improve a bit and, after few attempts, Chalmers team will become seriously competitive.

Bibliography

- [1] Sorensen Spazzafumo. *Hydrogen and fuel cells : Emerging technologies and applications*. Elsevier Science Technology, 2018 (cit. on pp. 8–11).
- [2] Dilip Sharma Vinod Singh Yadav S.L. Soni. «Engine performance of optimized hydrogen-fueled direct injection engine». In: *Energy* (2013) (cit. on p. 12).
- [3] Geovane Prante Karsten Wittek Vitor Cogo. «Development of a pneumatic actuated low-pressure direct injection gas injector for hydrogen-fueled internal combustion engines». In: *International journal of hydrogen energy* (2022) (cit. on pp. 12–14).
- [4] K. Yamane. «Hydrogen Fueled ICE, Successfully Overcoming Challenges through High Pressure Direct Injection Technologies: 40 Years of Japanese Hydrogen ICE Research and Development». In: *SAE International* (2018) (cit. on p. 12).
- [5] M. Schumacher and M. Wensing. «Investigations on an Injector for a Low Pressure Hydrogen Direct Injection». In: *SAE International* (2014) (cit. on p. 13).
- [6] et al. O’Hayre Ryan. *Fuel Cell Fundamentals*. John Wiley Sons, Incorporated, 2016 (cit. on pp. 14–19, 21, 22).
- [7] *Technical Rules of the Monaco race energy class* (cit. on pp. 23, 24, 33, 50, 57, 58).
- [8] <https://energyboatchallenge.com/challenge/races/> (cit. on pp. 24, 55, 57).
- [9] <https://plm.sw.siemens.com/en-US/simcenter/systems-simulation/amesim> (cit. on pp. 26, 49).
- [10] *DEA 1.0 Fuel cell system installation, operation and maintenance manual* (cit. on pp. 27–29, 36, 42, 43, 68).
- [11] *Sigracet whitepaper* (cit. on pp. 27, 31, 33).
- [12] *Orion fans datasheet, model OD254AP IP68 series* (cit. on p. 30).
- [13] A HydroComp Technical Report, Report 135; 2003-2007, HydroComp Inc. (cit. on p. 49).

BIBLIOGRAPHY

- [14] peter van Vlaardigen J Bakker. «Wetted surface area of recreational boats». In: *National Institute for public health and the Environment* (2018) (cit. on pp. 52, 53).